

Moderní experimentální metody

Elektronová spektroskopie a mikroskopie IV

Elektronová mikroskopie

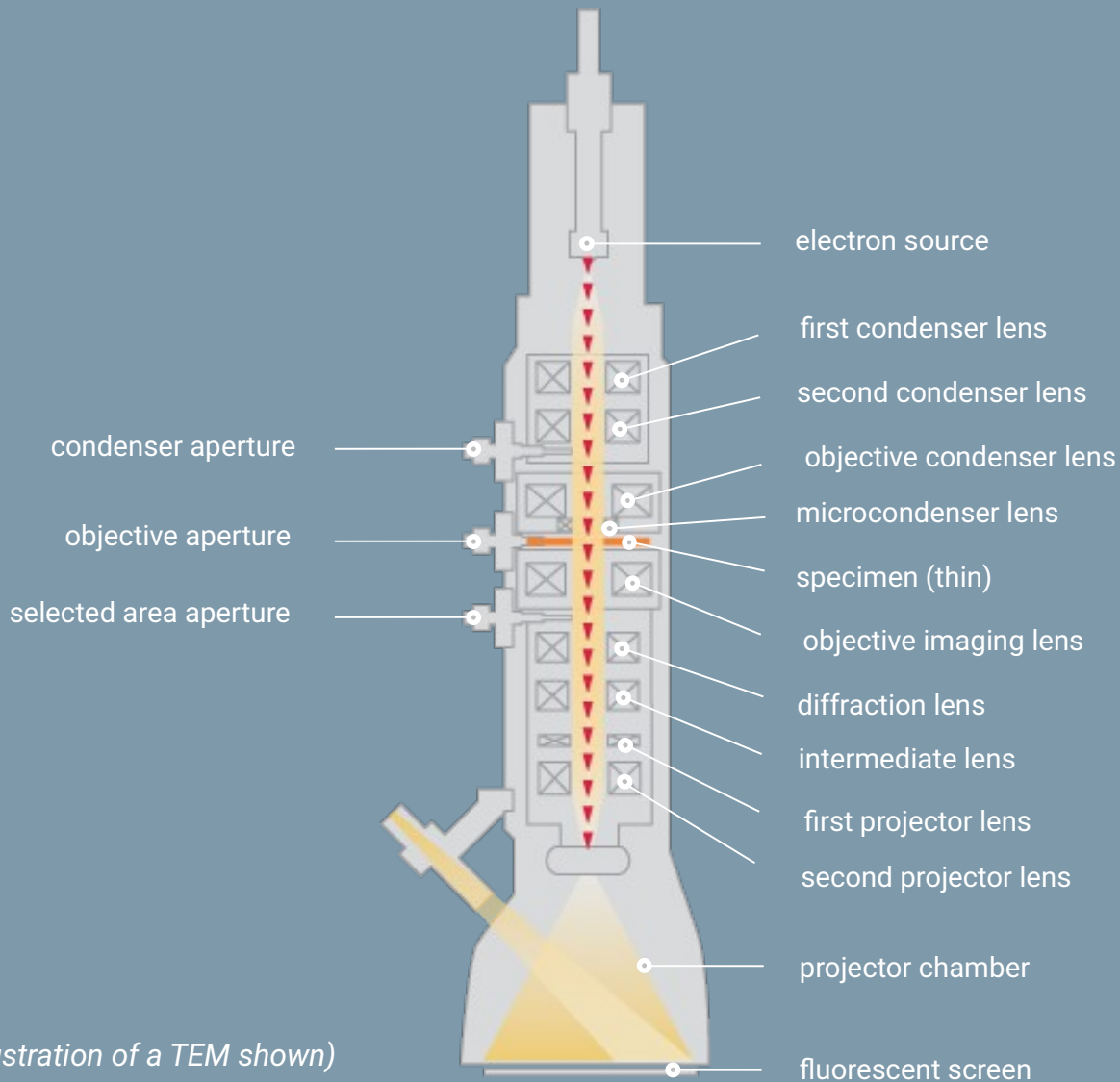
- Transmisní
- Rastrovací
- Běžné přidružené analytické metody
 - EDS, WDS
 - EELS
- Elektronová difrakce
 - EBSD
 - LEED
 - RHEED

History of electron microscopy

- First transmission electron microscopy
Ernst Ruska 1931
- First Czechoslovak electron microscope
– Armin Delong late 1940's
- Scanning electron microscopy
– Zvorykin 1942
- Aberation corrected electron microscopy
– atomic resolution
– Ondrej Krivanek 1970s



Basic Microscope Classifications



Charged
particle
microscope

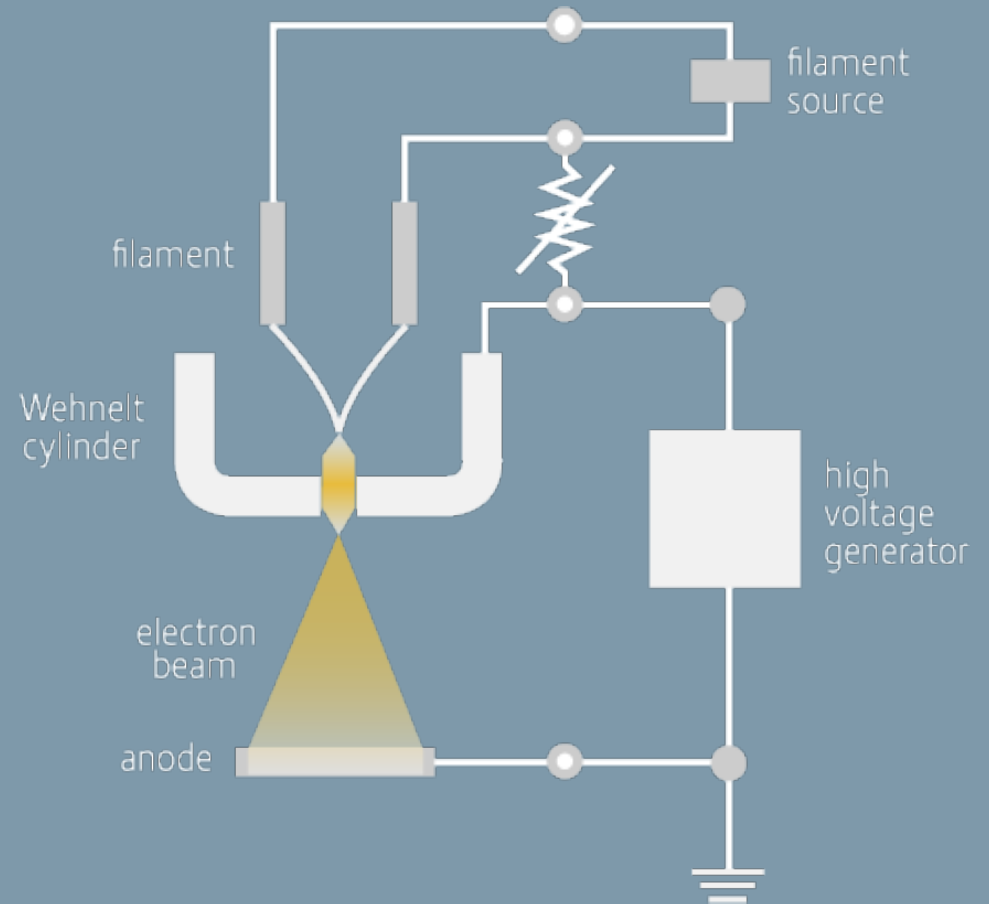
(Illustration of a TEM shown)

Comparing Microscopes

	LIGHT MICROSCOPE	ELECTRON MICROSCOPE
<i>The source of illumination</i> ▶	The ambient light source is light for the microscope	Electrons are used to “see” – light is replaced by an electron gun built into the column
<i>The lens type</i> ▶	Glass lenses	Electromagnetic lenses
<i>Magnification method</i> ▶	Magnification is changed by moving the lens	Focal length is changed by changing the current through the lens coil
<i>Viewing the sample</i> ▶	Eyepiece (ocular)	Fluorescent screen or digital camera
<i>Use of vacuum</i> ▶	No vacuum	Entire electron path from gun to camera must be under vacuum

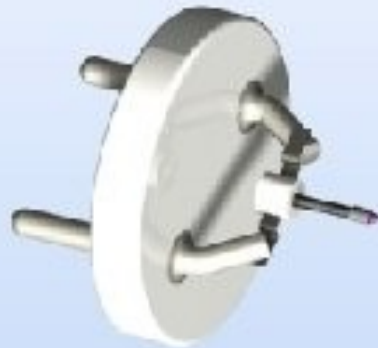
CORE TECHNOLOGY: The Electron Gun

- Three main sources of electrons:
 - Tungsten
 - LaB6 (lanthanum hexaboride)
 - Field Emission Gun (FEG)
- Different costs and benefits of each
- Each selected primarily for their brightness



Electron guns

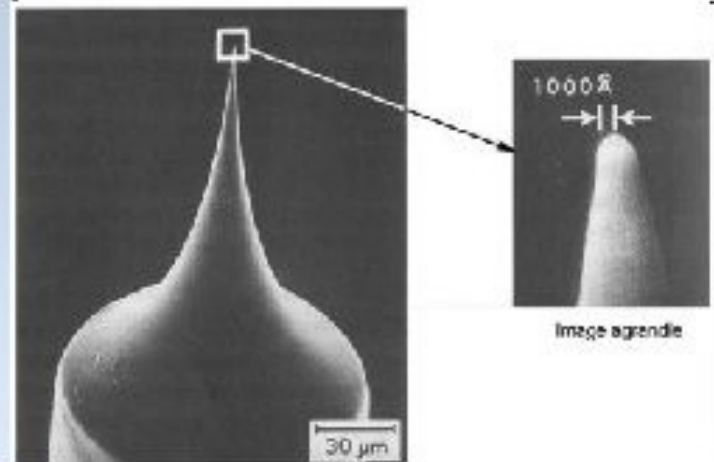
- With field emission guns we get a smaller spot and higher current densities compared to thermionic guns
- Vacuum requirements are tougher for a field emission guns



Single crystal of LaB₆

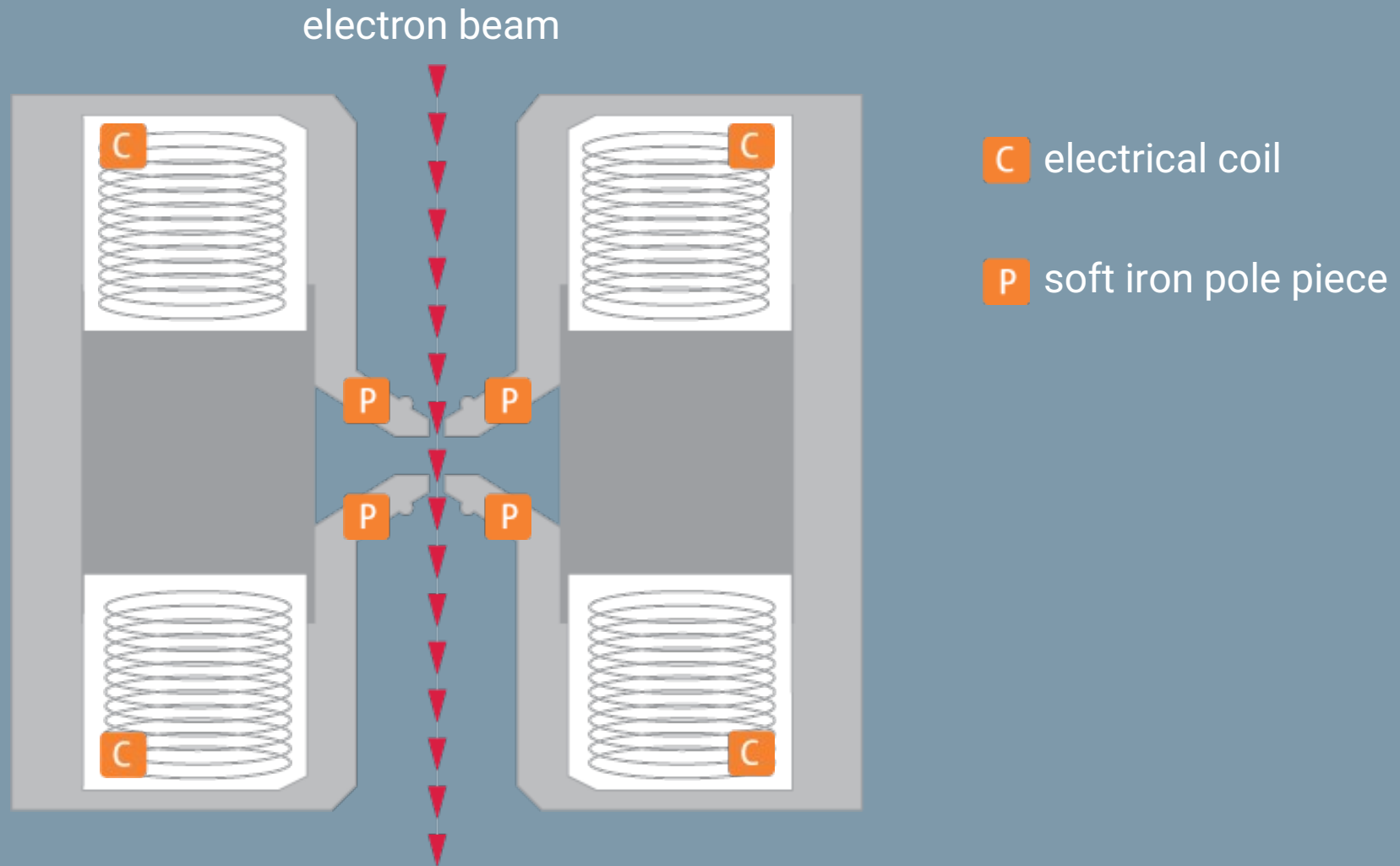


Tungsten wire

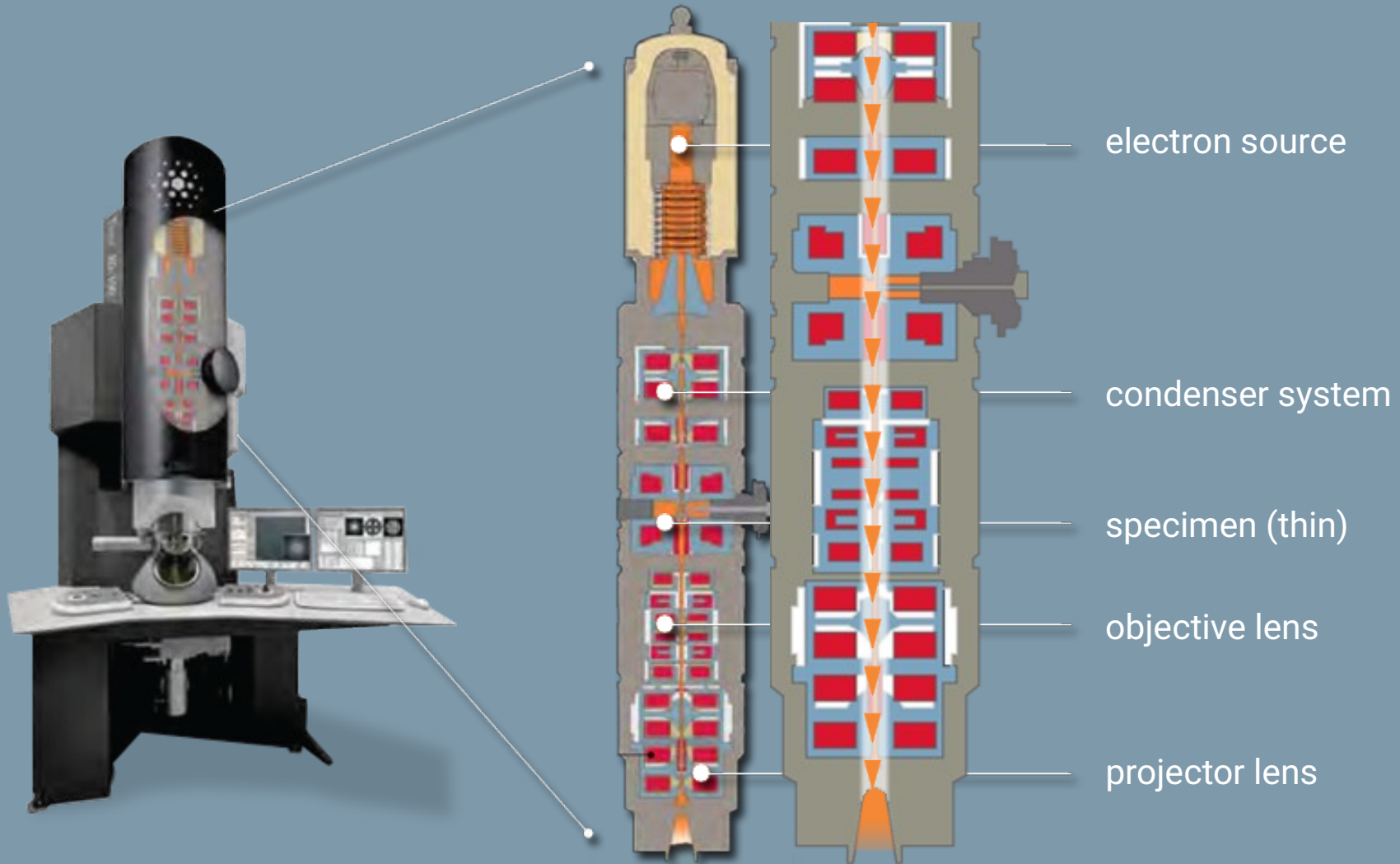


Field emission tip

CORE TECHNOLOGY: Electromagnetic Lenses



What is a Transmission Electron Microscope?



Electron microscopy

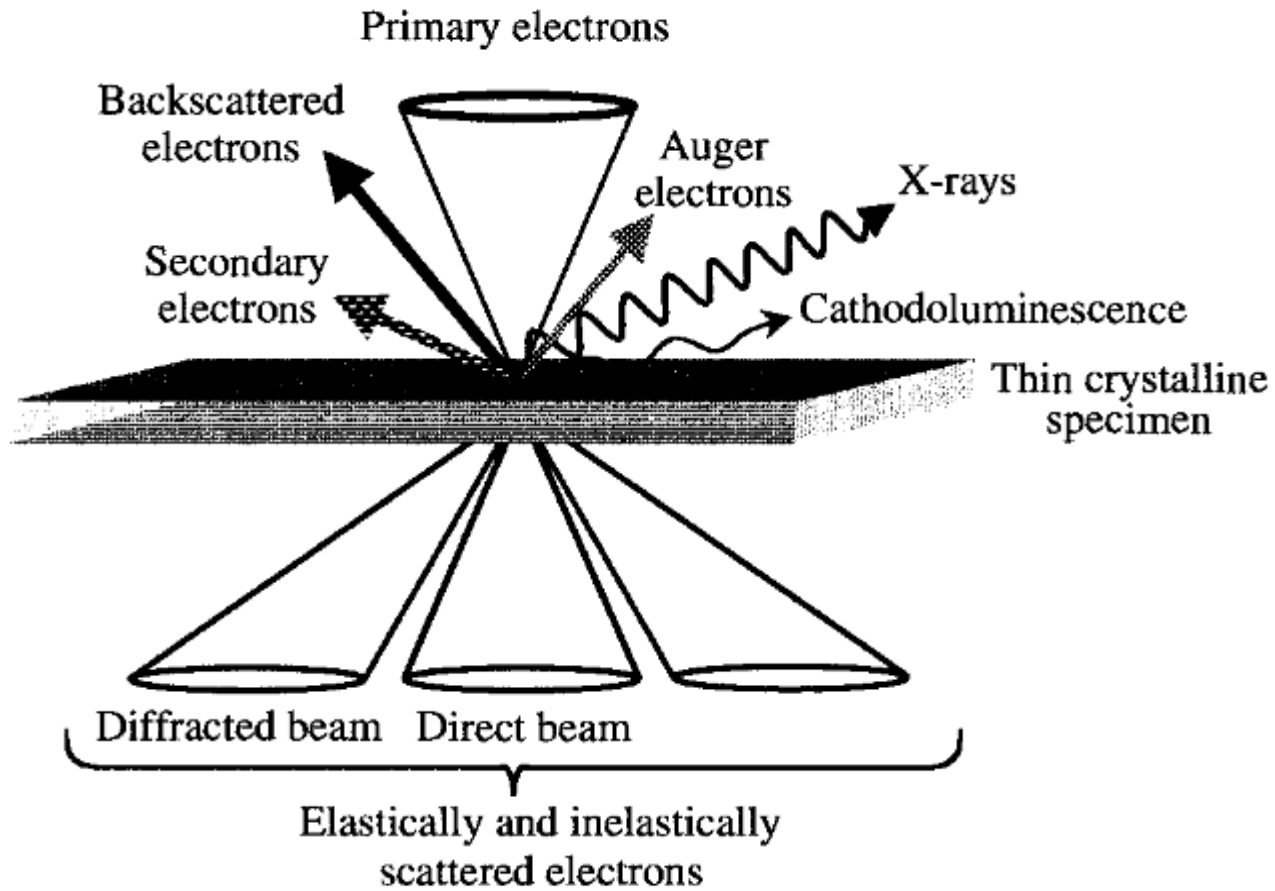


Fig. 2.31. Schematic diagram of the interactions between high-energy electrons and matter in TEM.

Electron microscopy

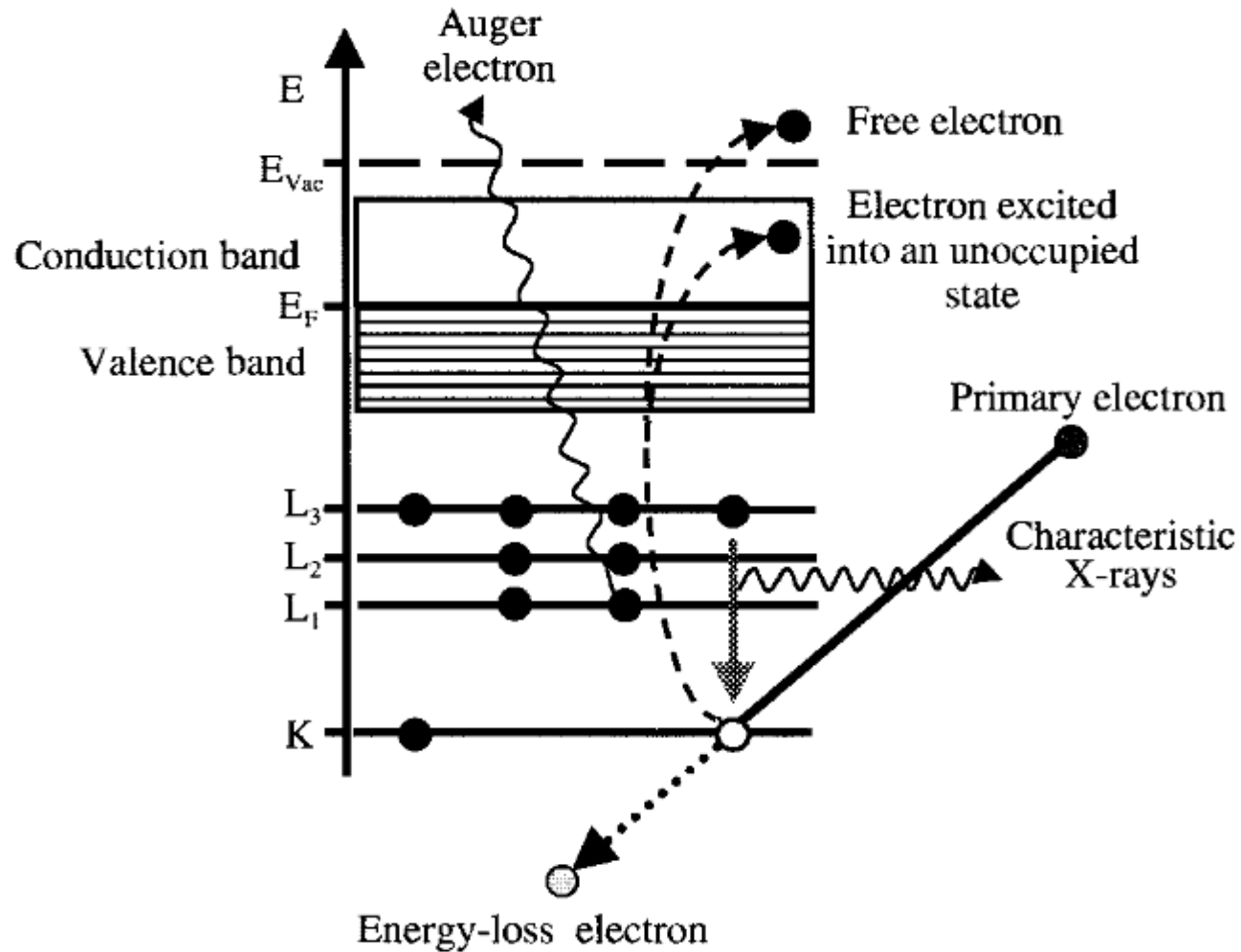
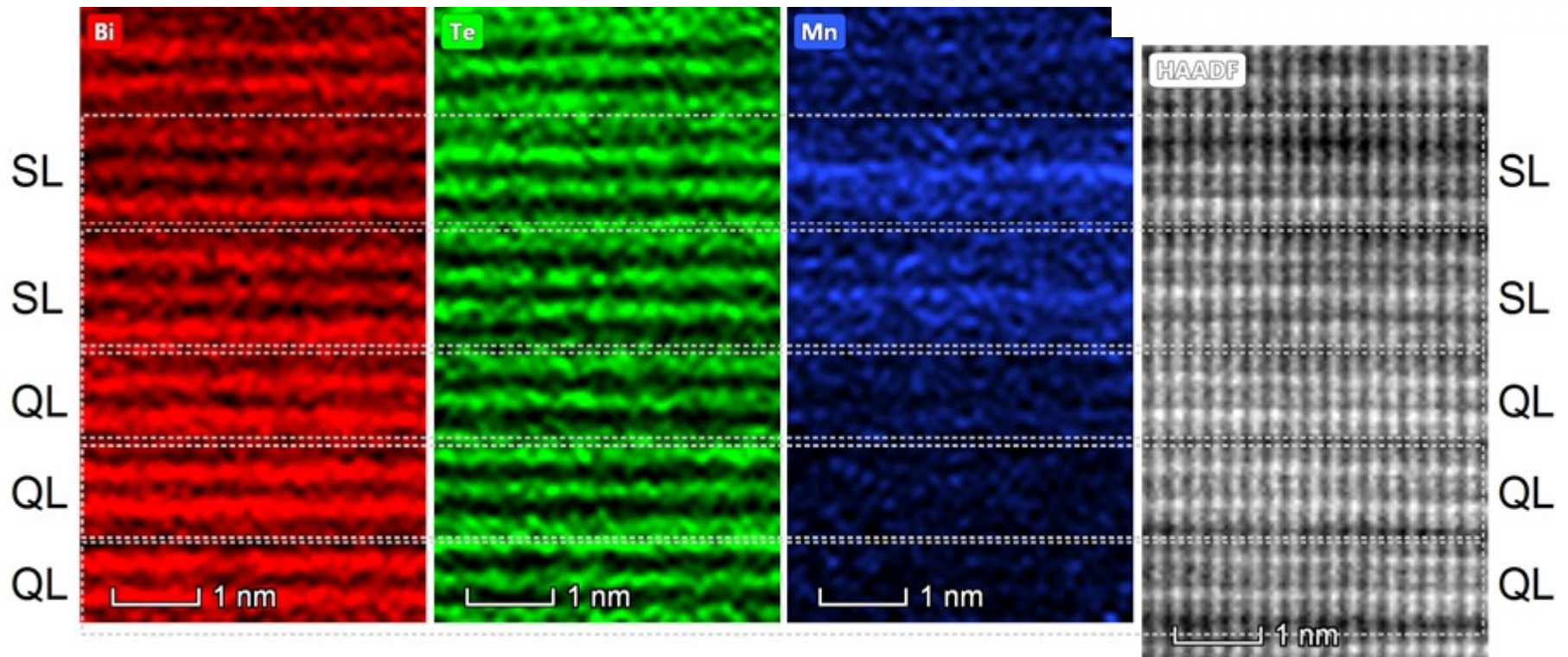
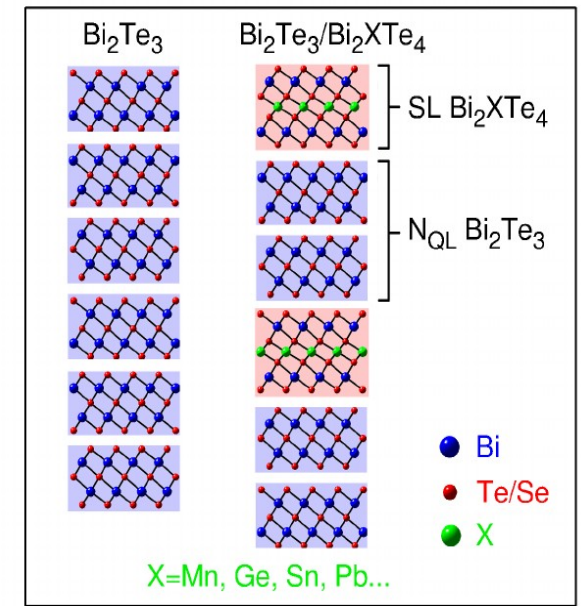


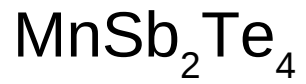
Fig. 2.32. Atomistic view of interaction processes between incident high-energy electrons and electrons of an individual atom.

JKU Linz, Graz
10% Mn Bi_2Te_3

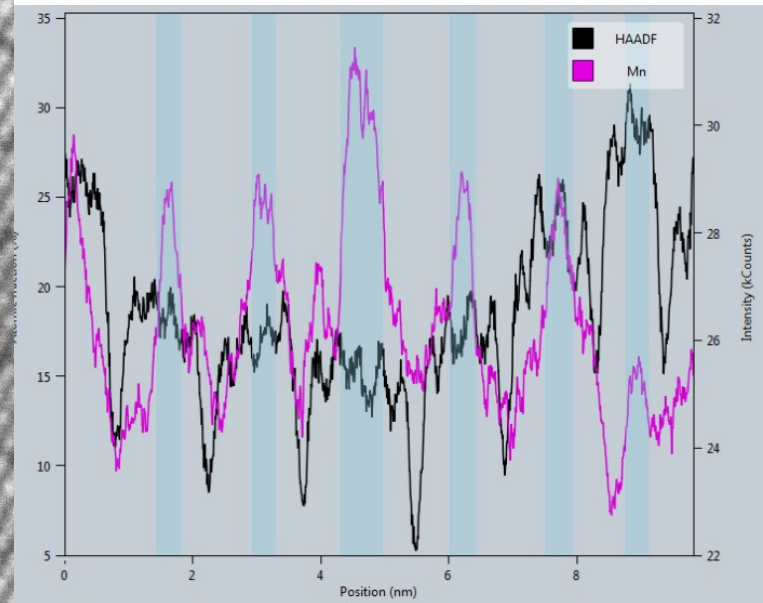
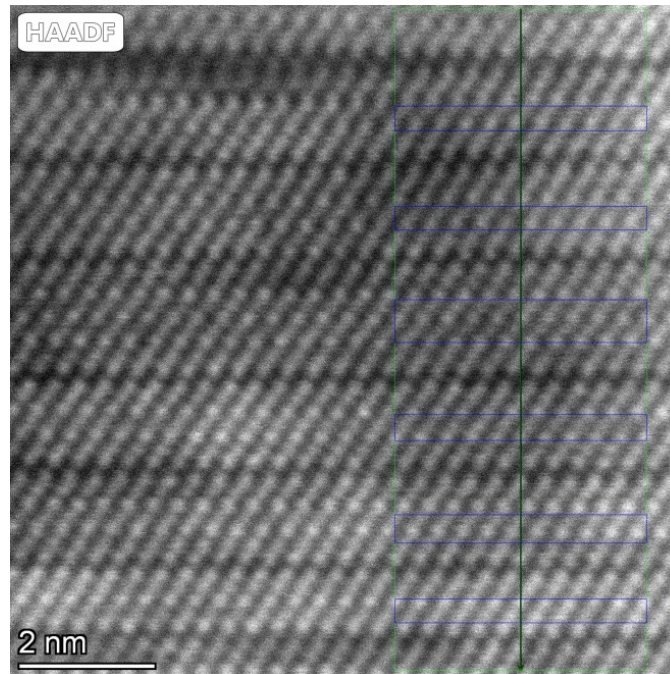
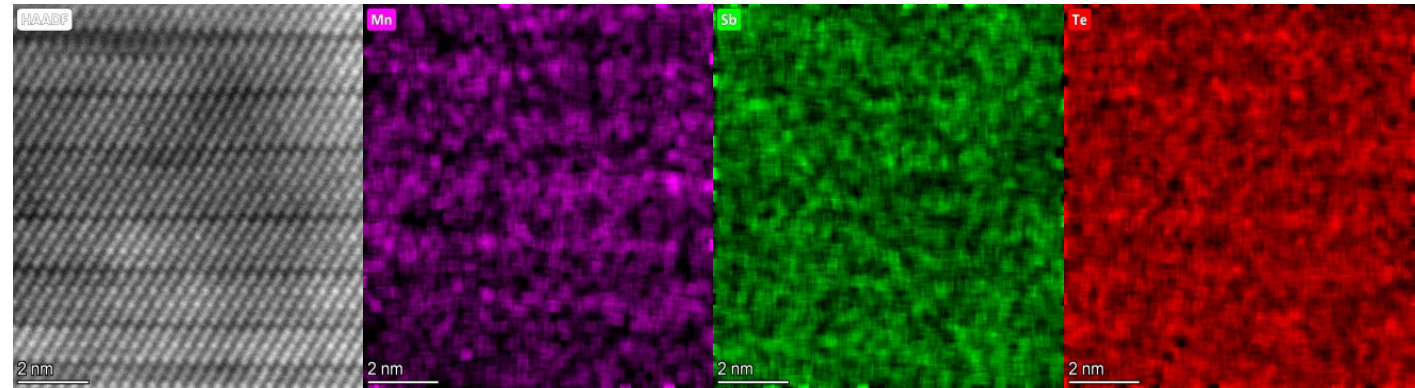
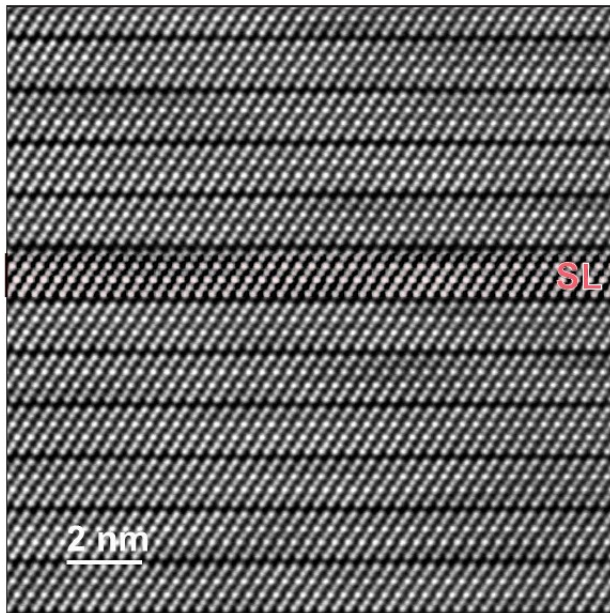
HAADF STEM



CEITEC Nano

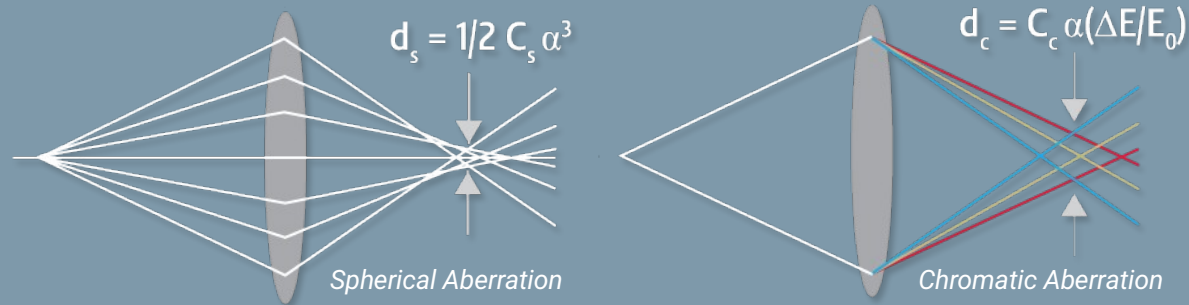


HAADF STEM



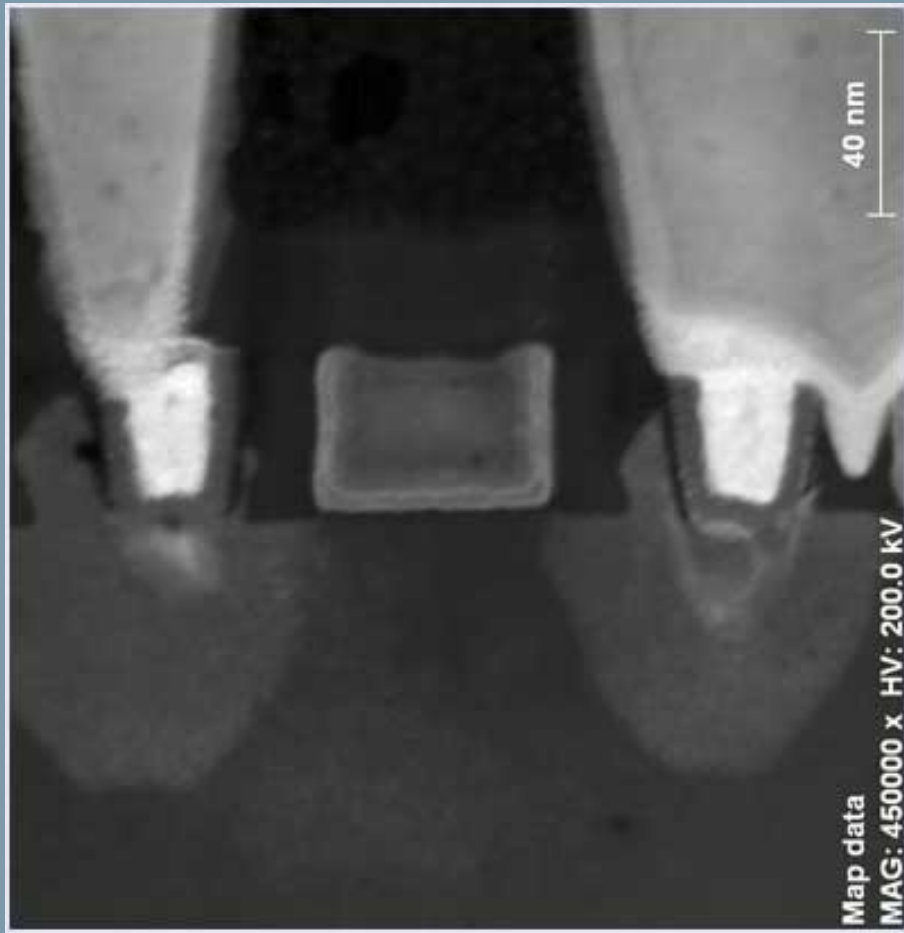
Defect nine atomic planes
Most probably
 $\text{Mn}_2\text{Sb}_2\text{Te}_5$

TEM Aberration Correction

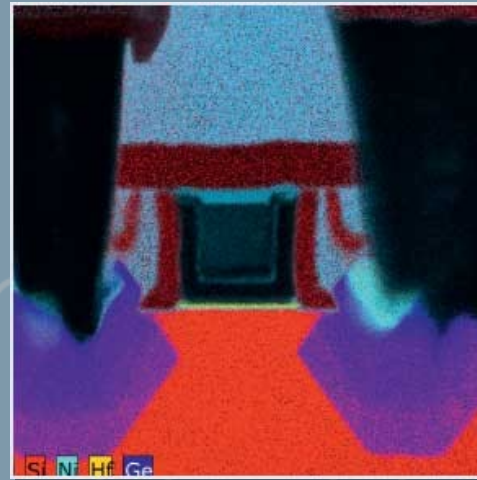


- Chromatic aberration is distortion that occurs when there is a failure of a lens to focus all colors (wavelengths) to the same convergence point.
 - Correcting the aberration is necessary, otherwise the resulting image would be blurry and delocalized, a form of aberration where periodic structures appear to extend beyond their physical boundaries.
 - Recent improvements in aberration correction have resulted in significantly-improved image quality and sample information.
- Spherical aberration occurs when parallel light rays that pass through the central region of the lens focus farther away than the light rays that pass through the edges of the lens.
 - Result is multiple focal points and a blurred image.

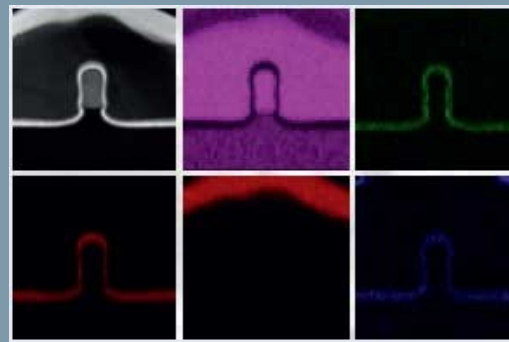
What is Scanning Transmission Electron Microscopy?



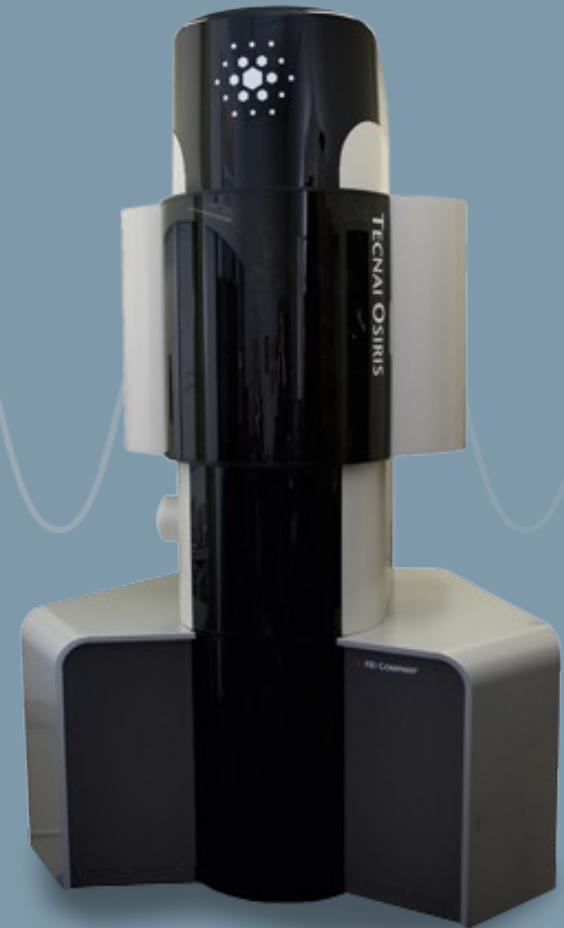
STEM image of a 32nm semiconductor device



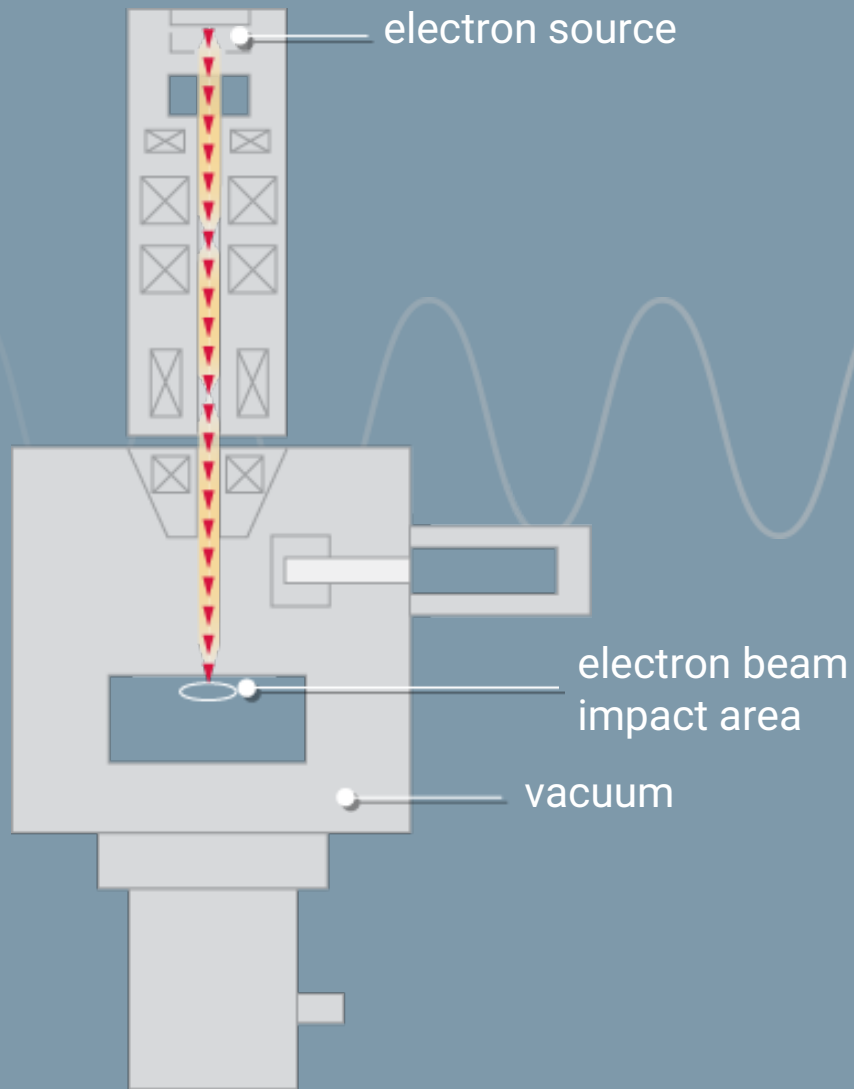
Elemental map of a 45 nm PMOS transistor structure



EDX map of semiconductor device



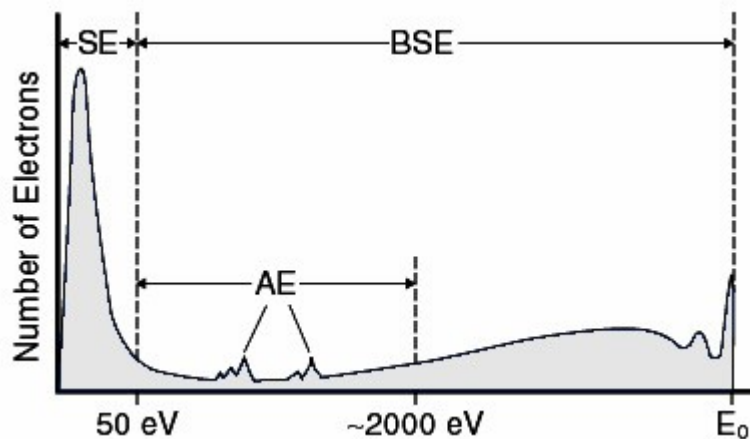
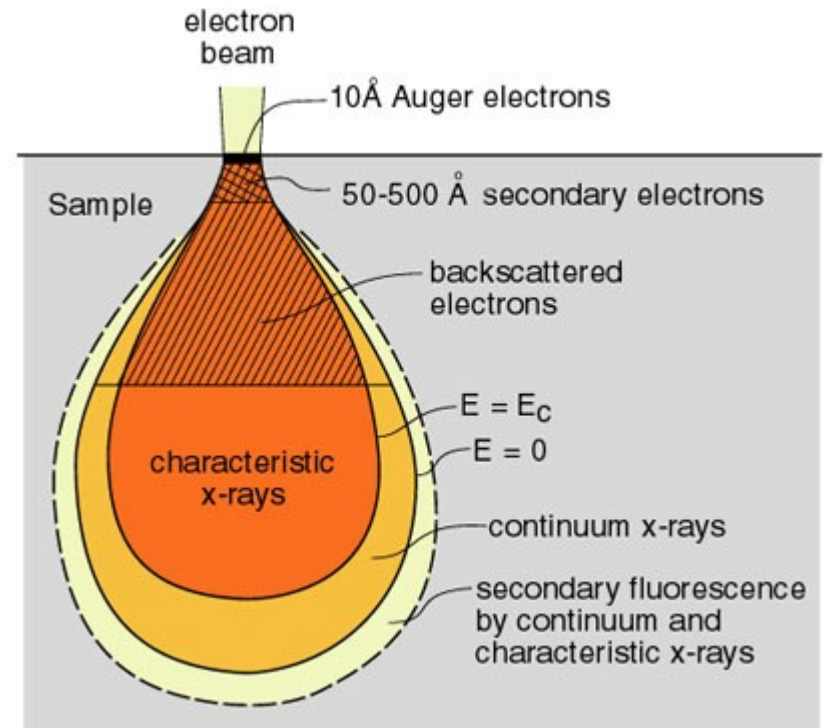
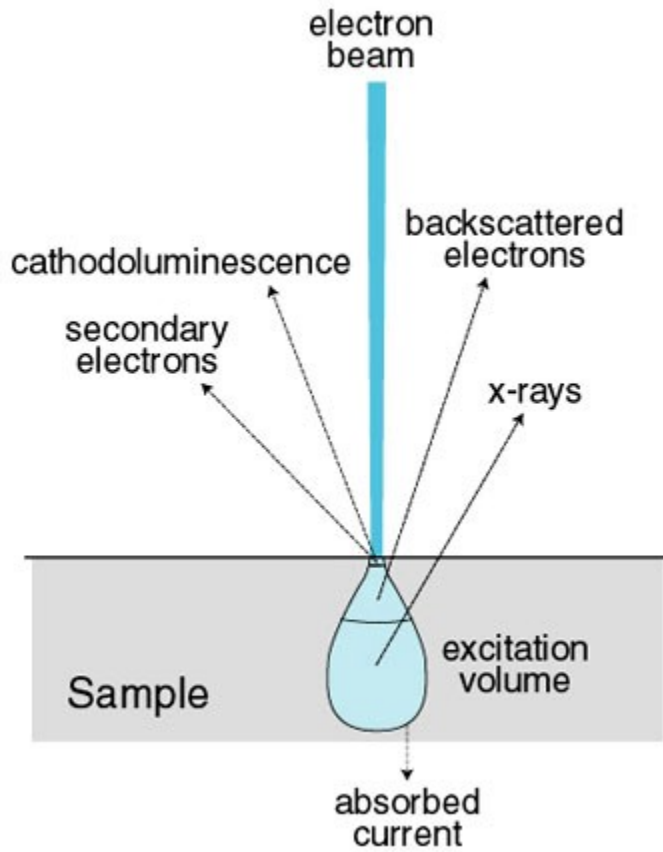
What is a Scanning Electron Microscope?



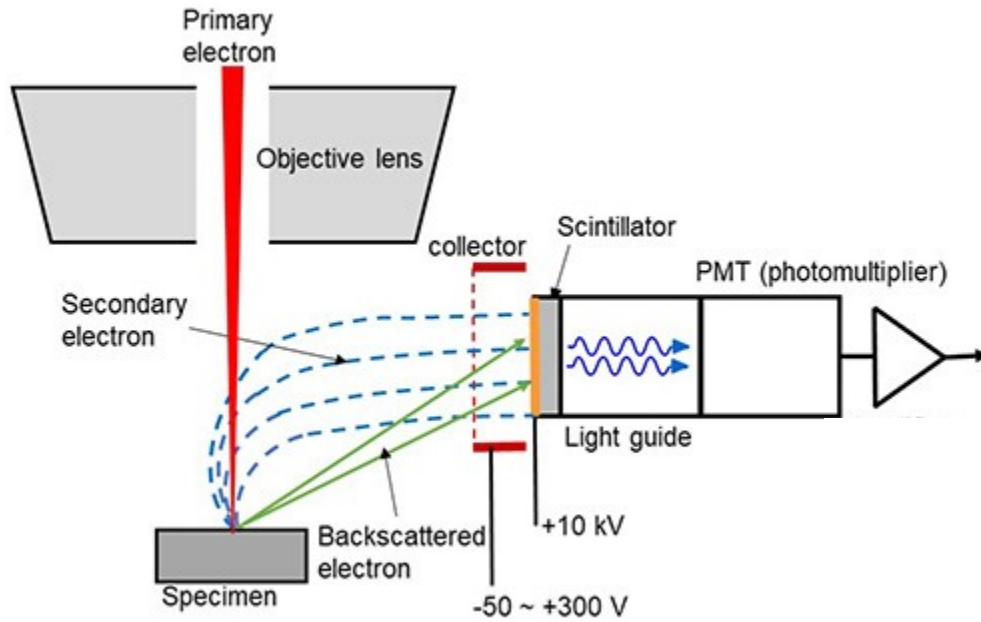
Comparing SEM and TEM

		TEM	SEM
<i>Electron Beam</i>	▶	Broad, static beams	Beam focused to fine point; sample is scanned line by line
<i>Voltages Needed</i>	▶	TEM voltage ranges from 60-300,000 volts	Accelerating voltage much lower; not necessary to penetrate the specimen
<i>Interaction of the beam electrons</i>	▶	Specimen must be very thin	Wide range of specimens allowed; simplifies sample preparation
<i>Imaging</i>	▶	Electrons must pass through and be transmitted by the specimen	Information needed is collected near the surface of the specimen
<i>Image Rendering</i>	▶	Transmitted electrons are collectively focused by the objective lens and magnified to create a real image	Beam is scanned along the surface of the sample to build up the image

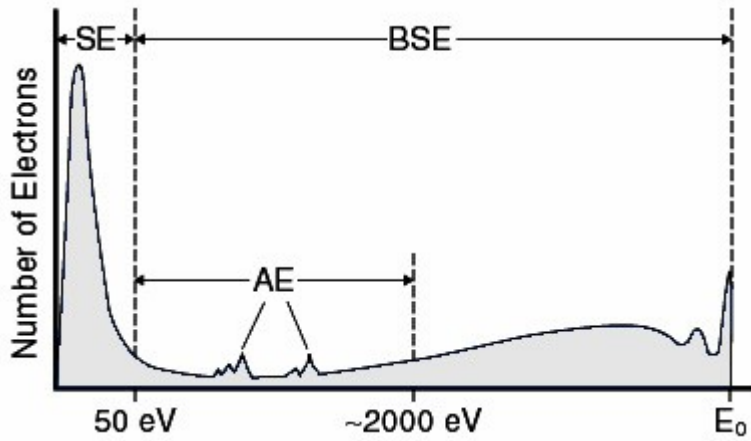
Electron microscopy



Electron microscopy



Detectors



Backscattered electron detector:
(Solid-State Detector)

Secondary electron detector:
(Everhart-Thornley)

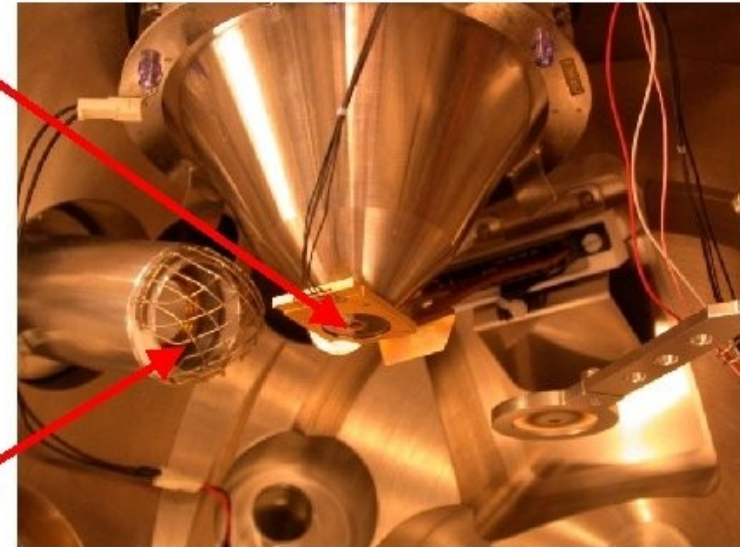
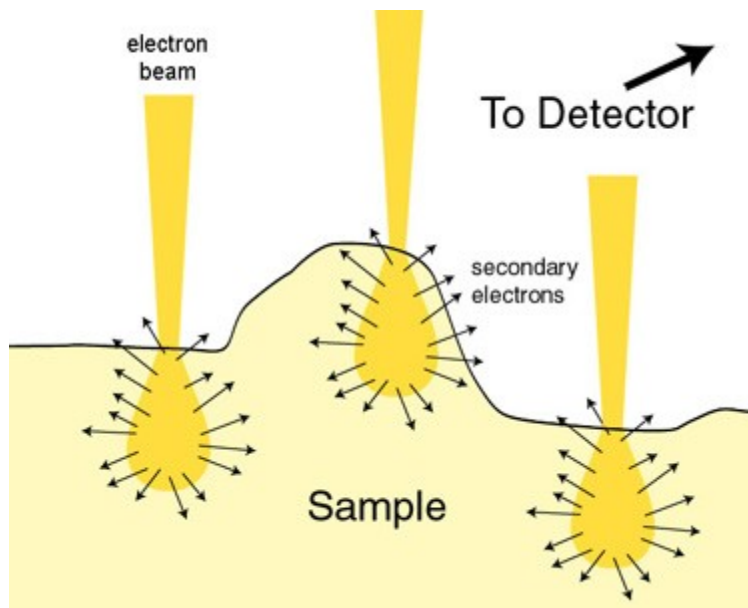


Image: Anders W. B. Skilbred, UiO

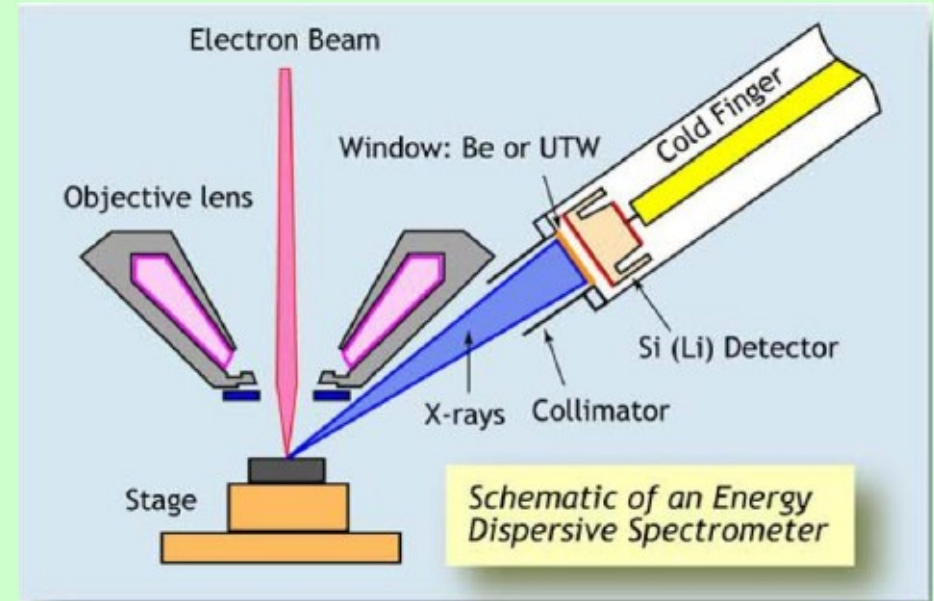
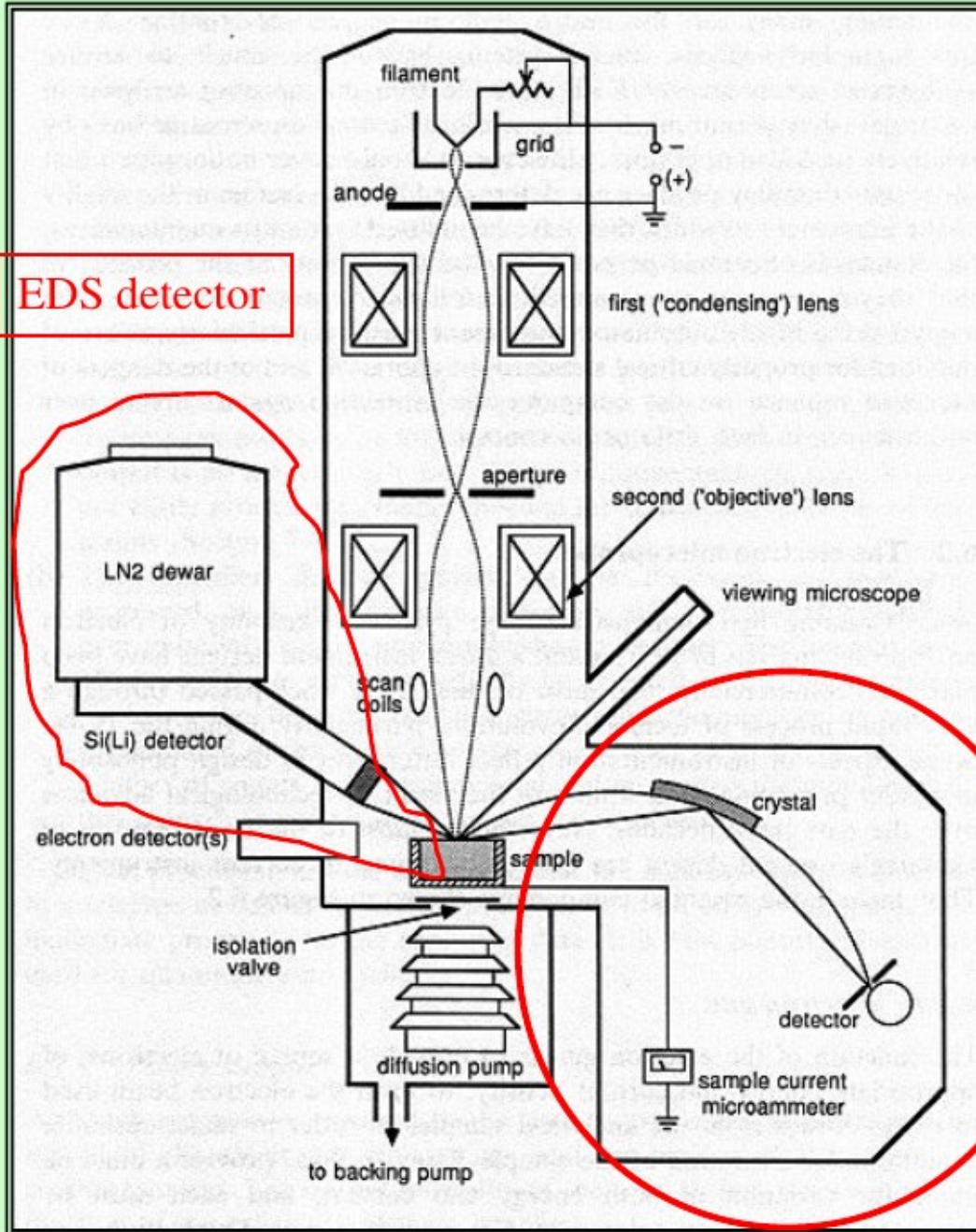
Electron microscopy



Sekundární elektrony – topografický kontrast

Zpětně odražené – chElectron microscopyický kontrast

Electron microscopy

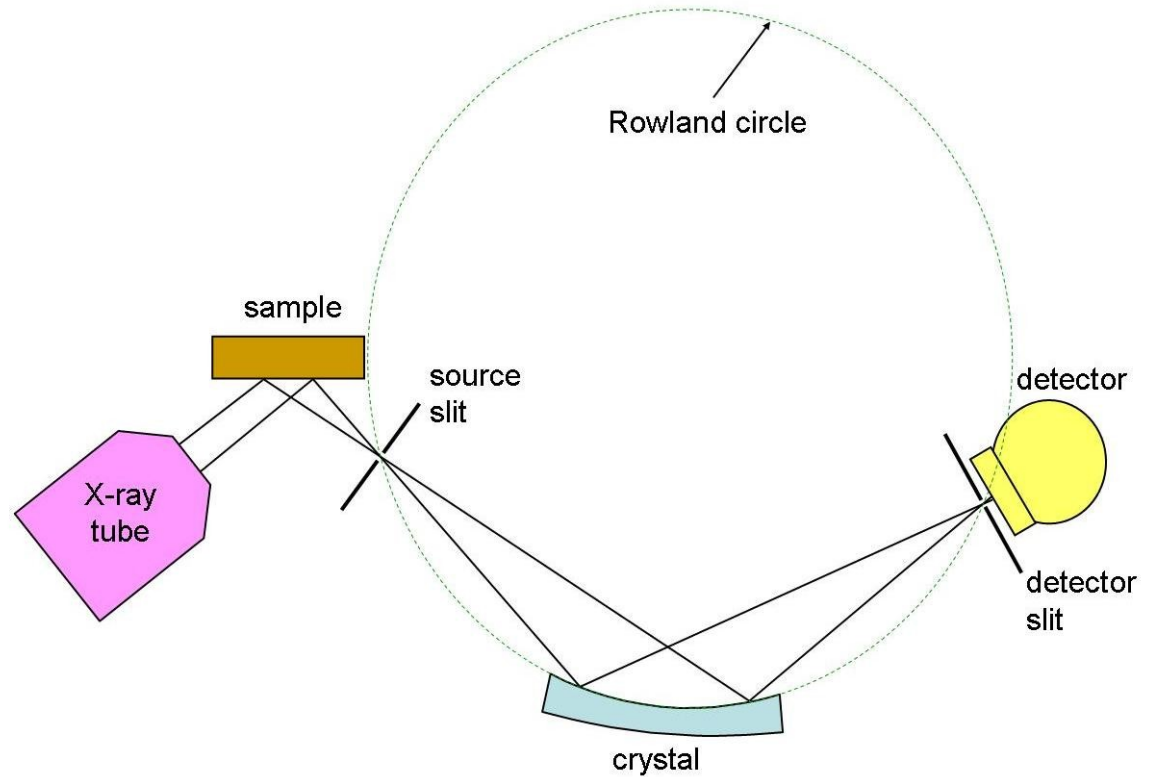
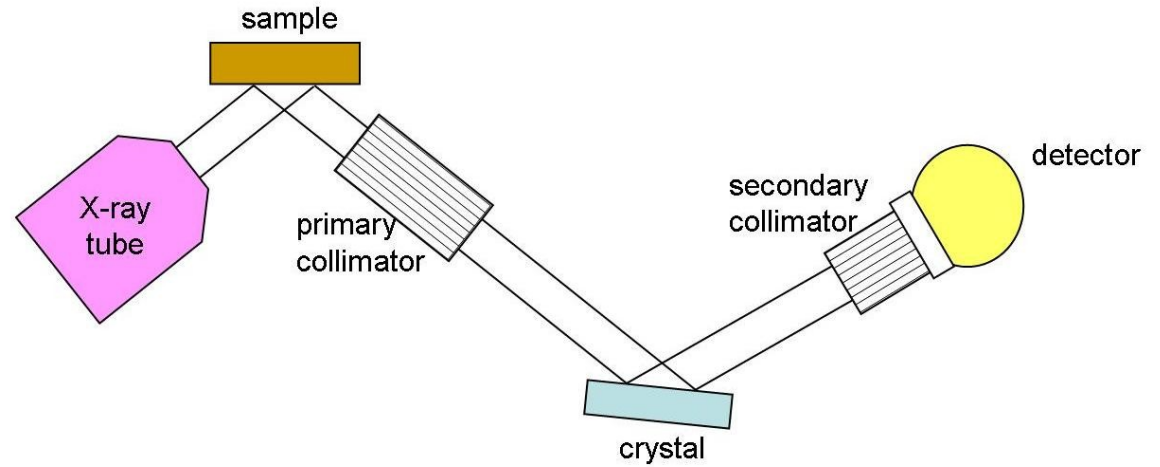


SEM combined with Energy dispersive spectrometer (EDS) and Wavelength Dispersive Spectrometer (WDS).

WDS spectrometers

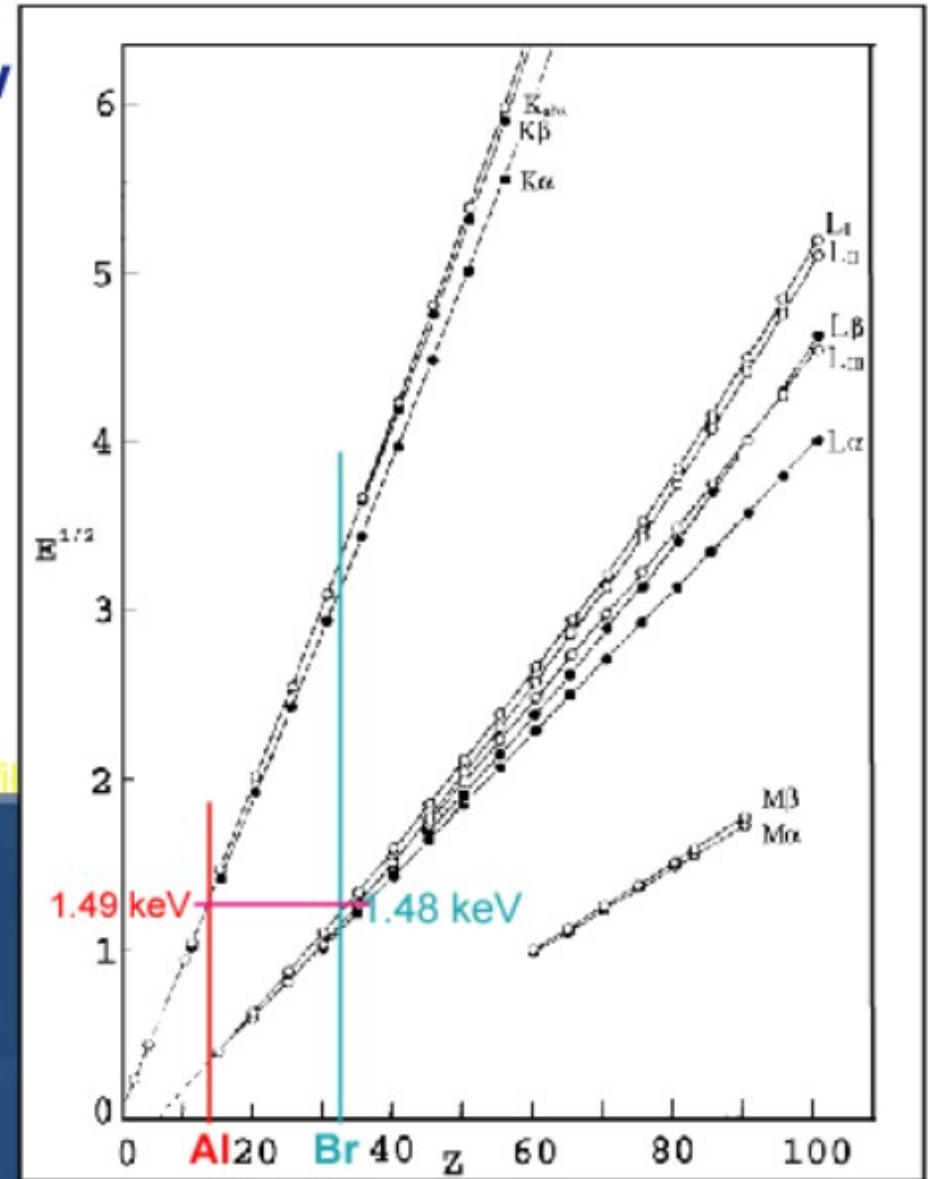
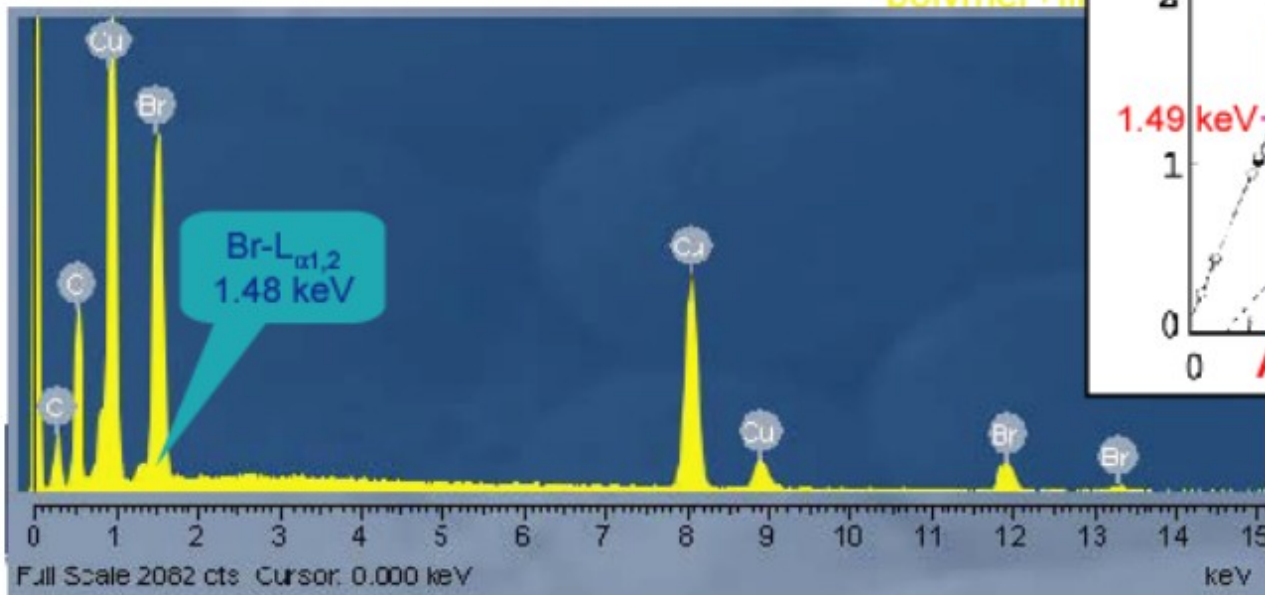
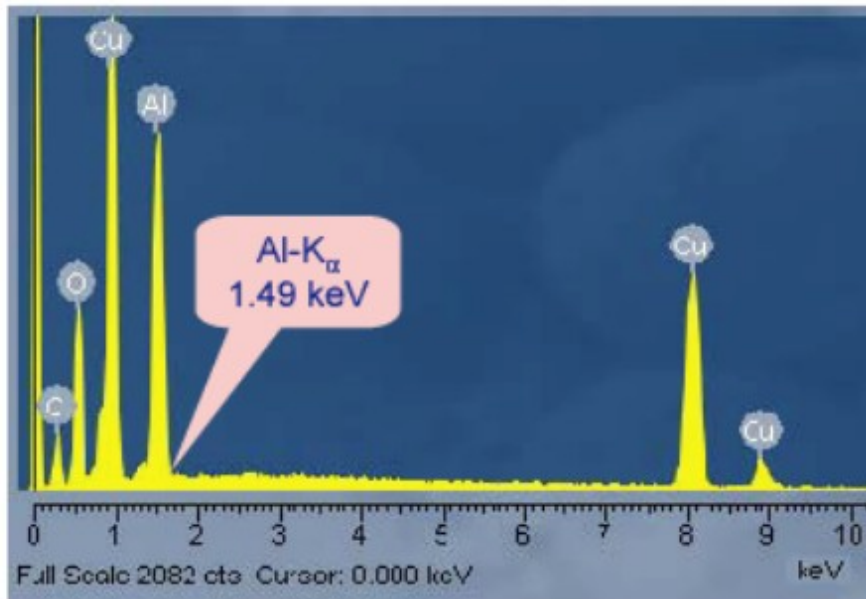
Electron microscopy

WDS:
better energy resolution
better precision
longer time



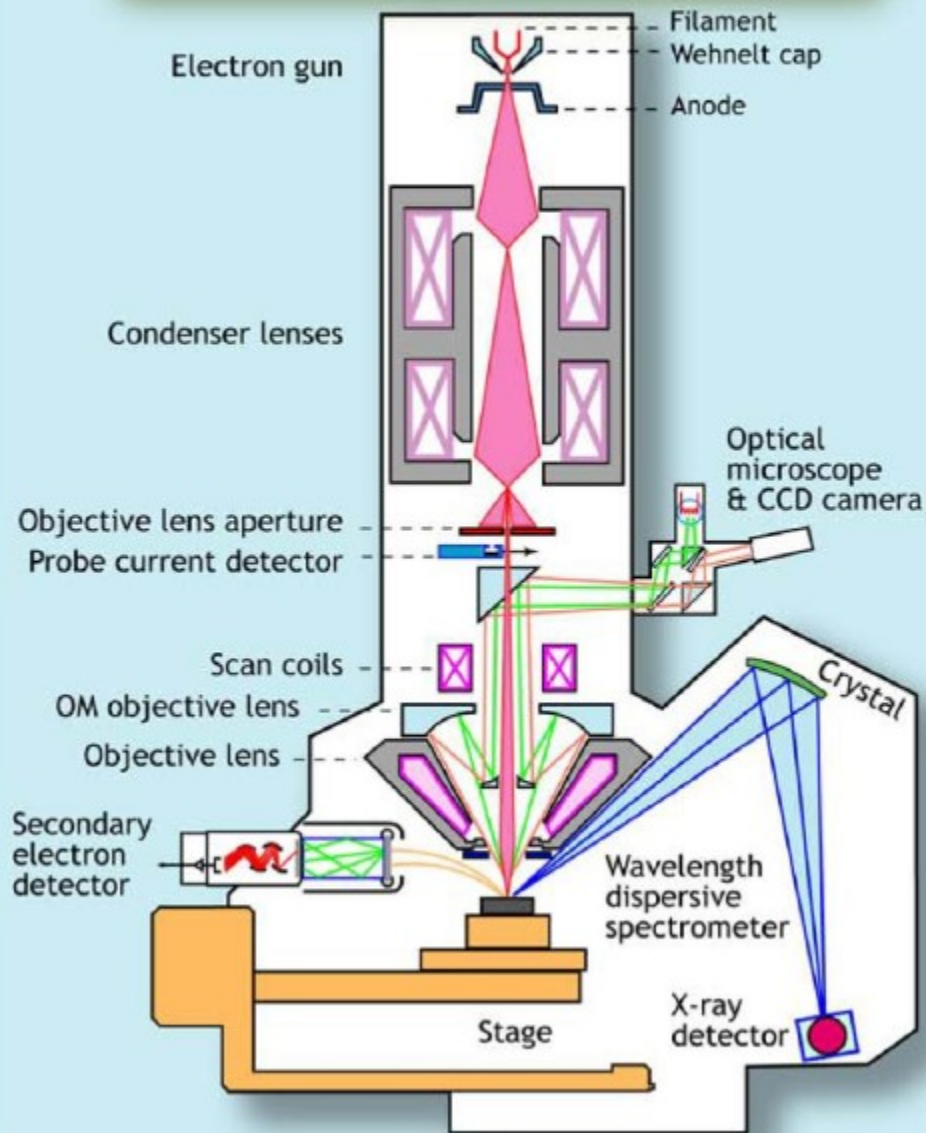
Electron microscopy

Characteristic lines: Moseley's Law

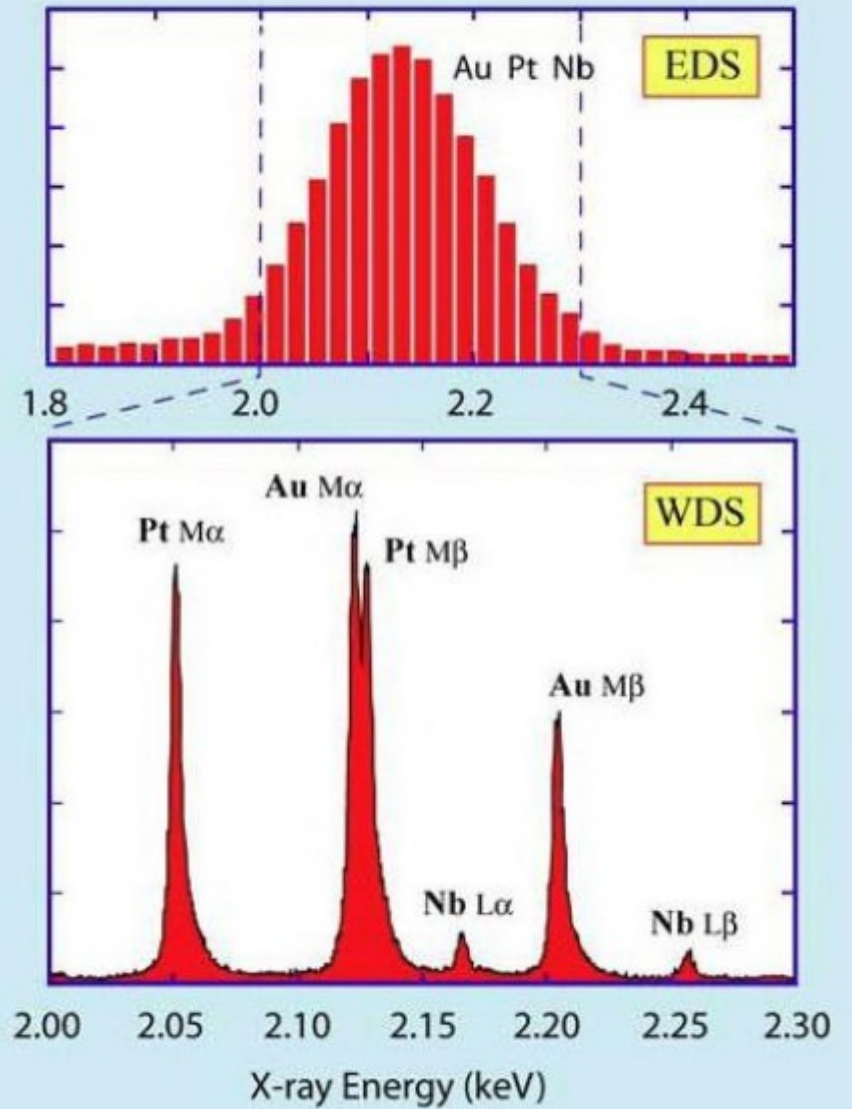


Electron microscopy

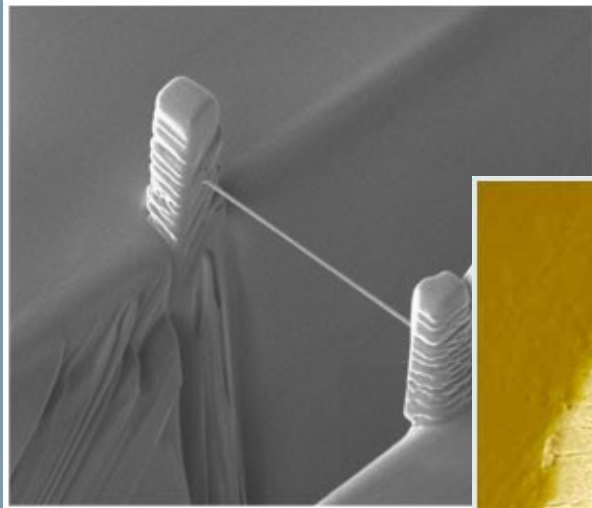
Schematic of an Electron Microprobe with a Wavelength Dispersive Spectrometer



Energy Resolution of EDS vs WDS



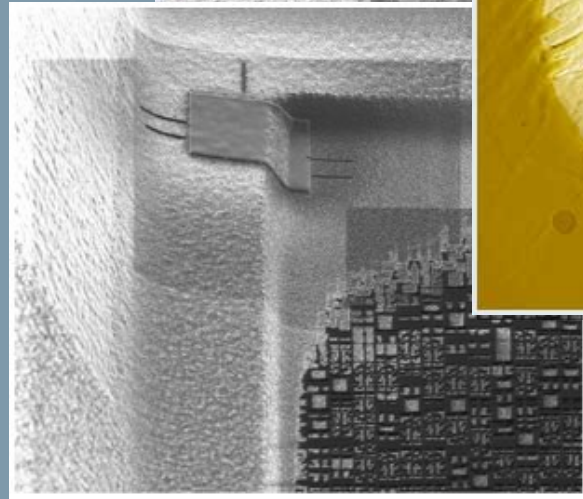
What is a Focused Ion Beam? (FIB)



Platinum Nano-Wire



FIB-cut in steel v2a FF by 1nA to
1B milling-002 steel
water imaged with a plasma FIB



Physical Failure Analysis



FEI V400ACE Focused Ion Beam

EELS

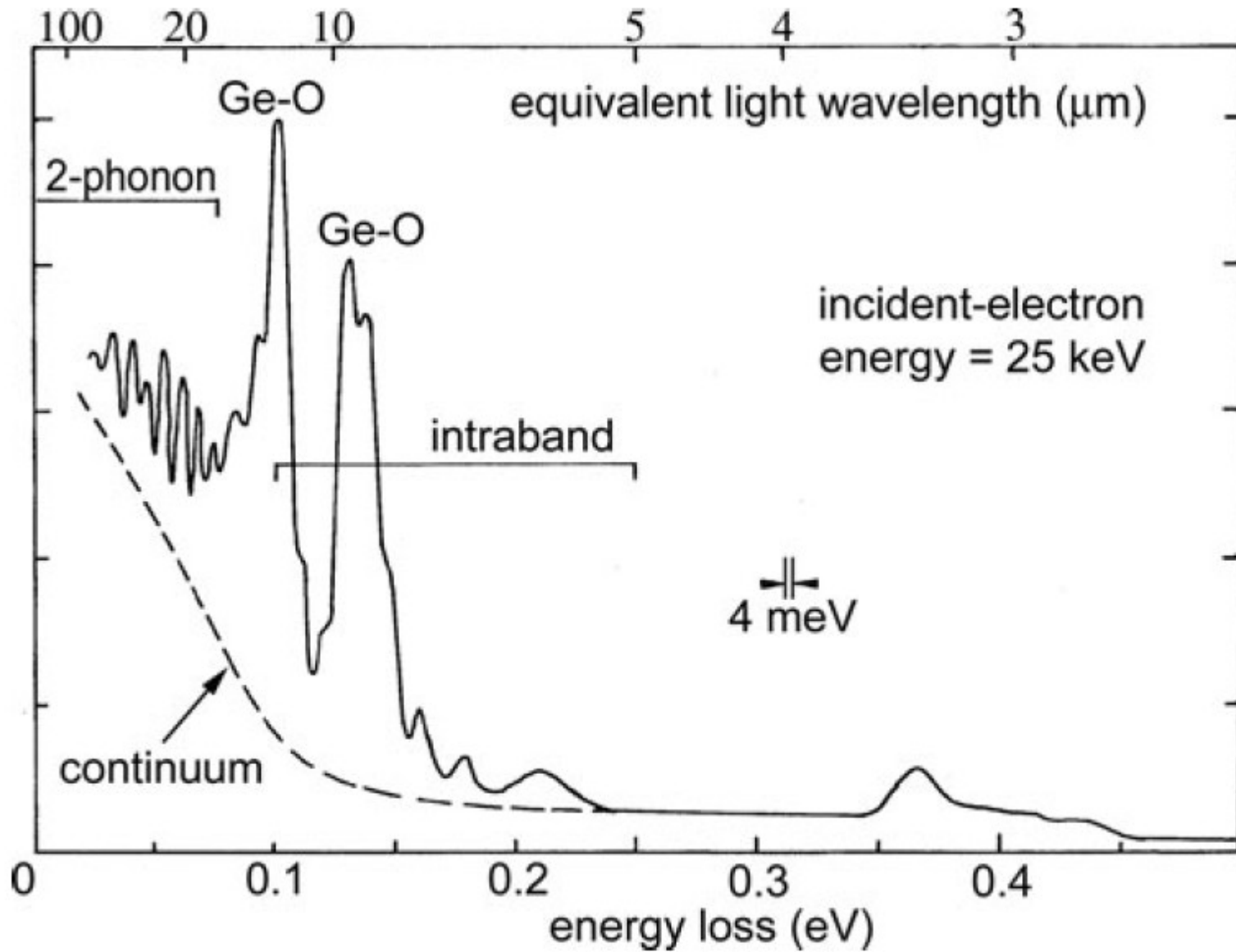


Fig. 1.9 Energy-loss spectrum of a 25-nm germanium film showing phonon and vibrational modes, as well as intraband electronic transitions (Schröder, 1972)

Electron microscopy

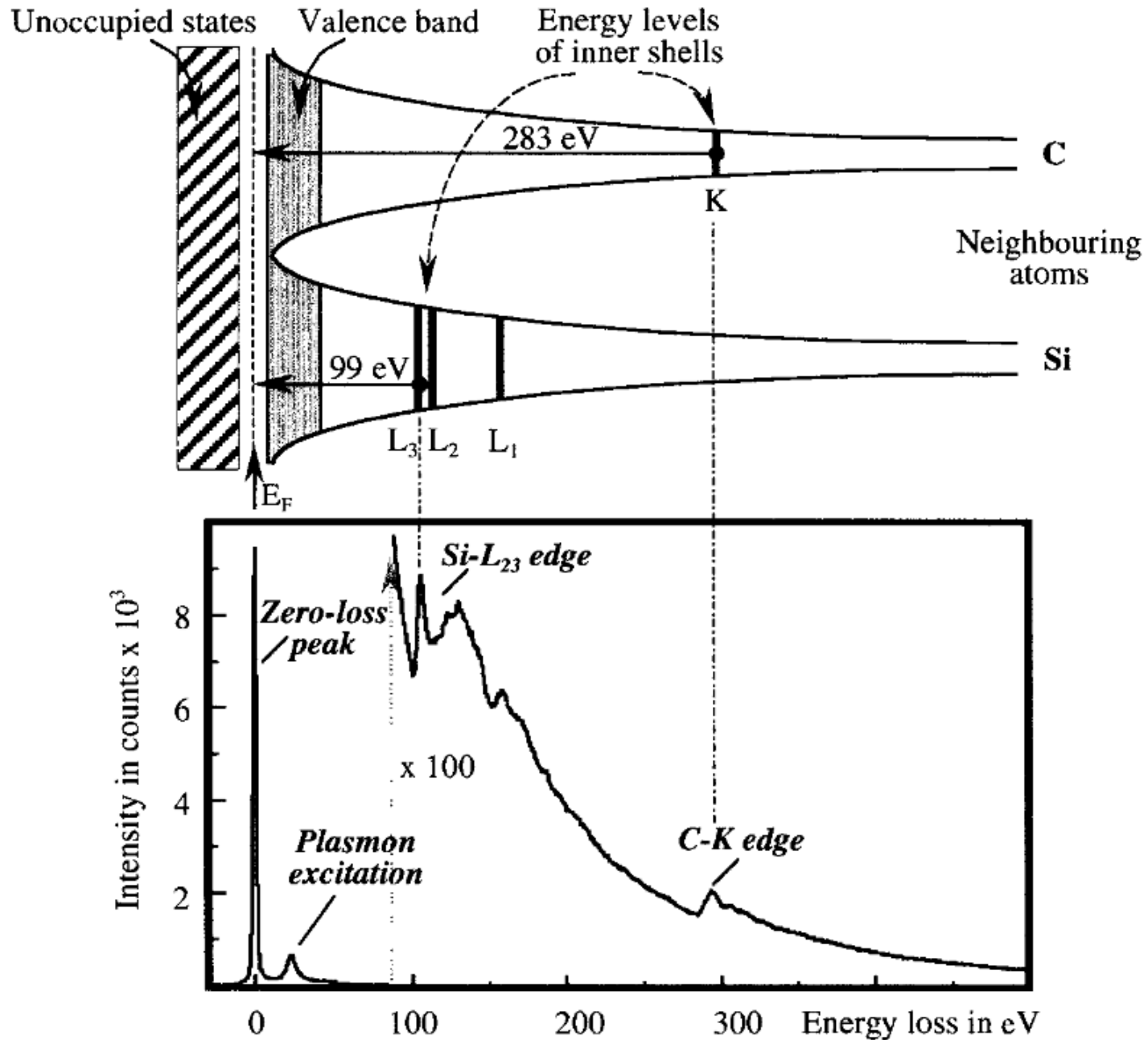
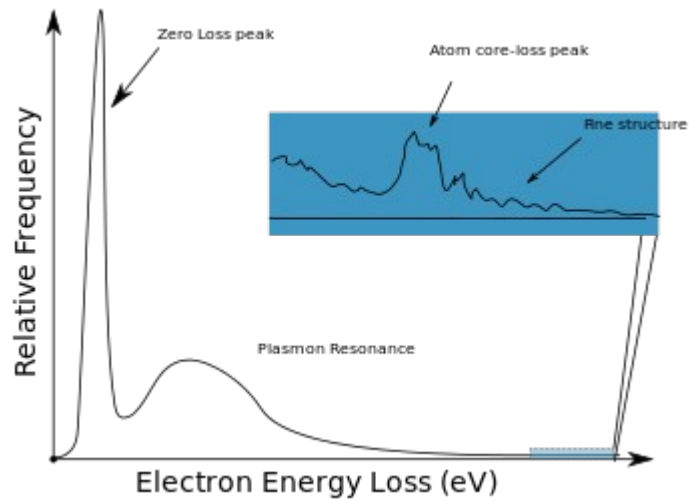
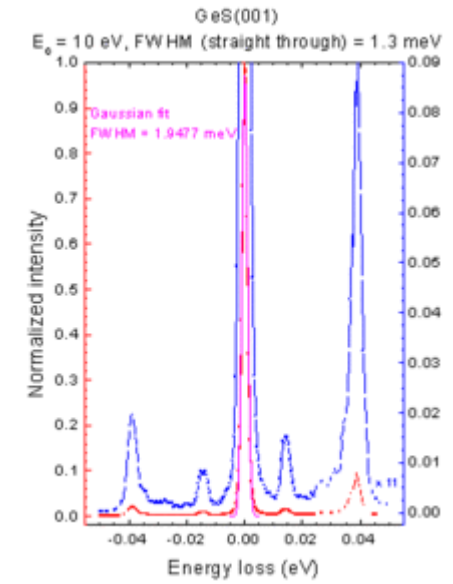
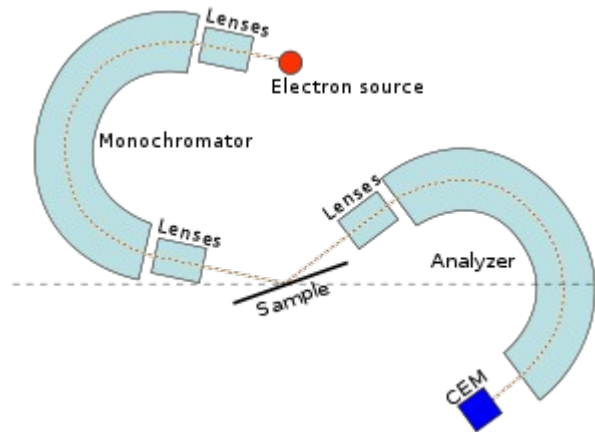


Fig. 2.35. Typical EEL spectrum and corresponding energy-level scheme.

EELS



EELS

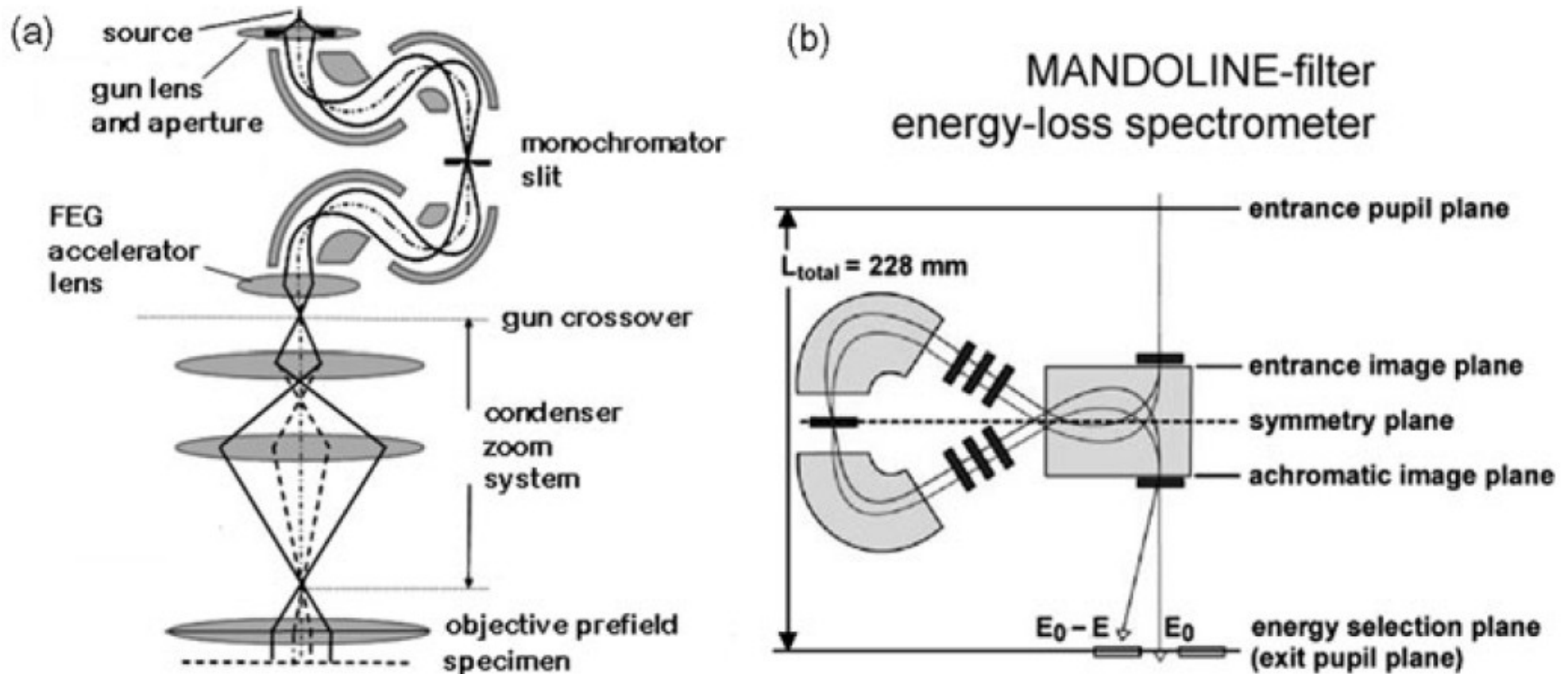


Fig. 2.32 Components of the Zeiss SESAM instrument: (a) electrostatic omega filter (dispersion $\approx 12 \mu\text{m}/\text{eV}$ at the midplane slit) and (b) MANDOLINE filter, whose dispersion at the energy-selecting plane exceeds $6 \mu\text{m}/\text{eV}$

EELS

Fig. 1.11 (a) X-ray emission spectrum recorded from an oxidized region of stainless steel, showing overlap of the oxygen *K*-peak with the *L*-peaks of chromium and iron. (b) Ionization edges are more clearly resolved in the energy-loss spectrum, as a result of the better energy resolution of the electron spectrometer (Zaluzec et al., 1984). From Zaluzec et al. (1984), copyright San Francisco Press, Inc., with permission

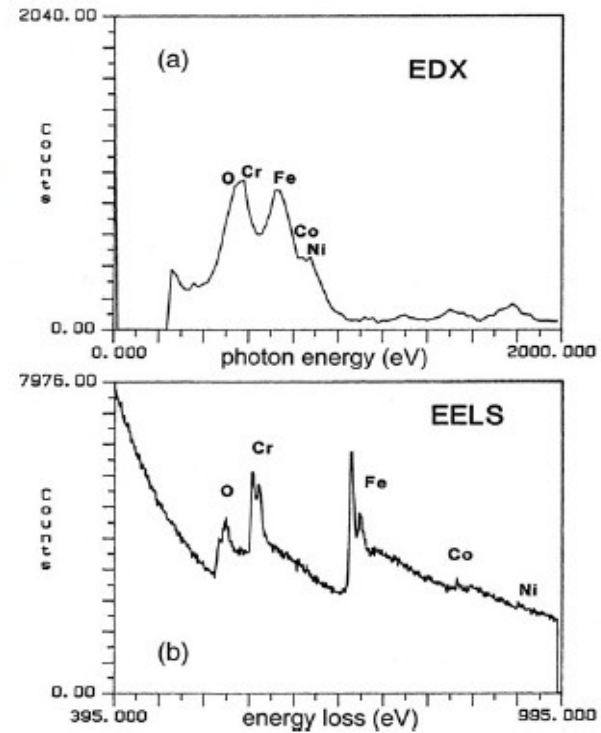
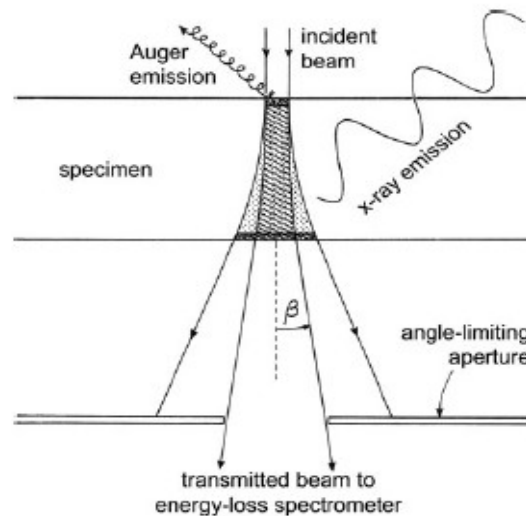


Fig. 1.12 Spreading of an electron beam within a thin specimen. X-rays are emitted from the *dotted region*, whereas the energy-loss spectrum is recorded from the *hatched region*, the spectrometer entrance aperture having a collimating effect. Auger electrons are emitted within a small depth adjacent to each surface



EELS

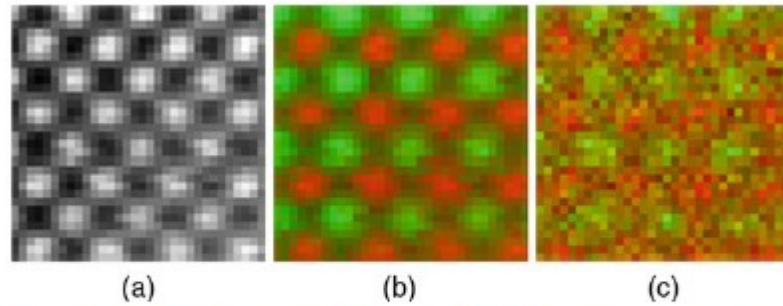


Fig. 1.14 (a) HAADF-STEM image of a [100]-projected GaAs specimen, showing bright Ga and As atomic columns. (b) EELS image showing the Ga-L₂₃ intensity in *green* and As-L₂₃ intensity in *red*. (c) EDX spectroscopy image with Ga-K α intensity in *green* and As-K α intensity in *red*. Courtesy of M. Watanabe

EELS

Fig. 3.7 Angular dependence of the differential cross sections for elastic and inelastic scattering of 100-keV electrons from a carbon atom, calculated using the Lenz model (Eqs. (3.50), (3.7), and (3.15)). Shown along the horizontal axis are (from left to right) the characteristic, median, mean, root-mean-square and effective cutoff angles for total inelastic scattering, evaluated using Eqs. (3.53), (3.54), (3.55), and (3.56)

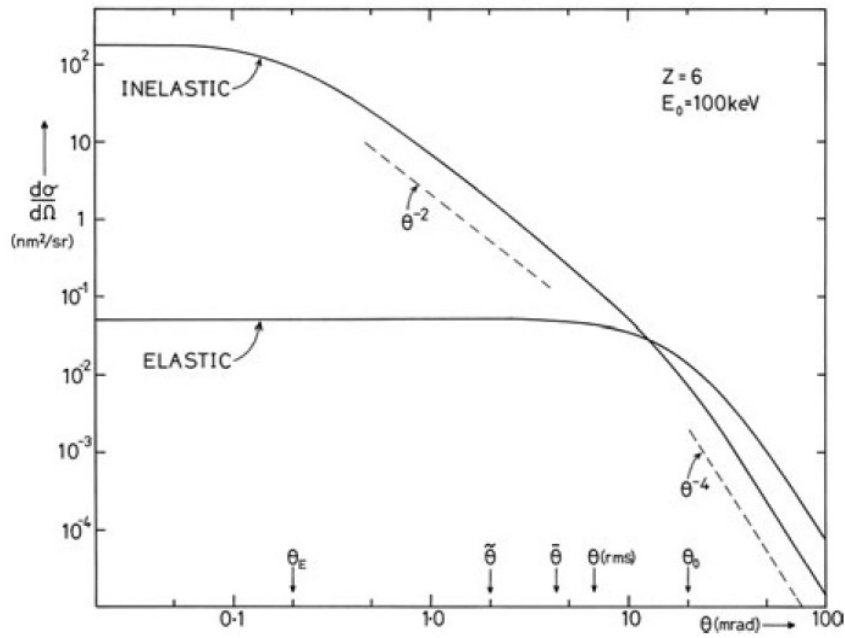
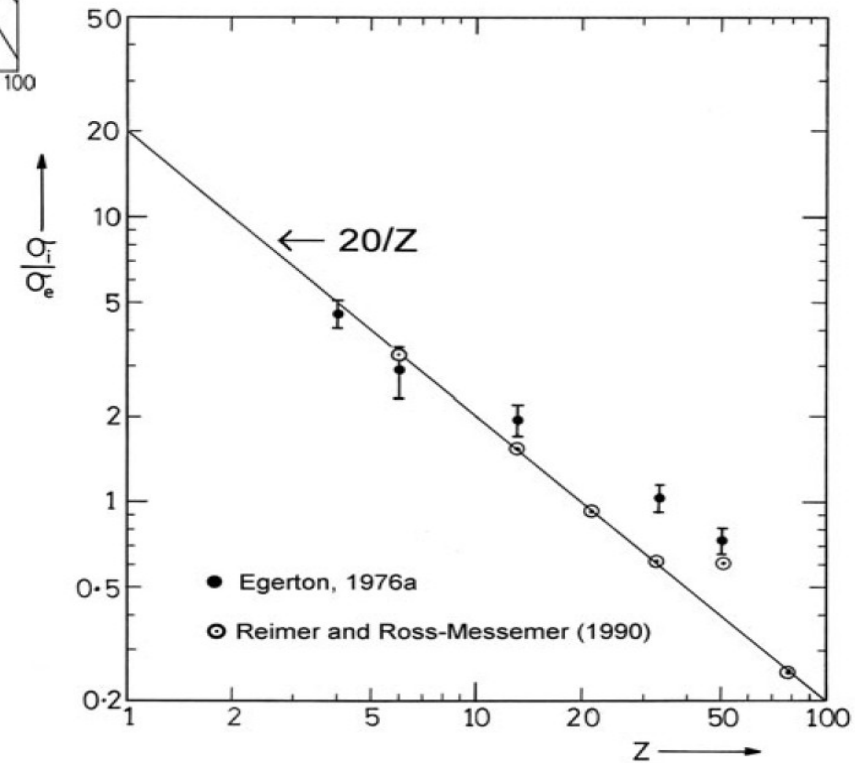


Fig. 3.8 Measured values of inelastic/elastic scattering ratio for 80-keV electrons, as a function of atomic number of the specimen. The *solid line* represents Eq. (3.18) with $C = 20$



EELS

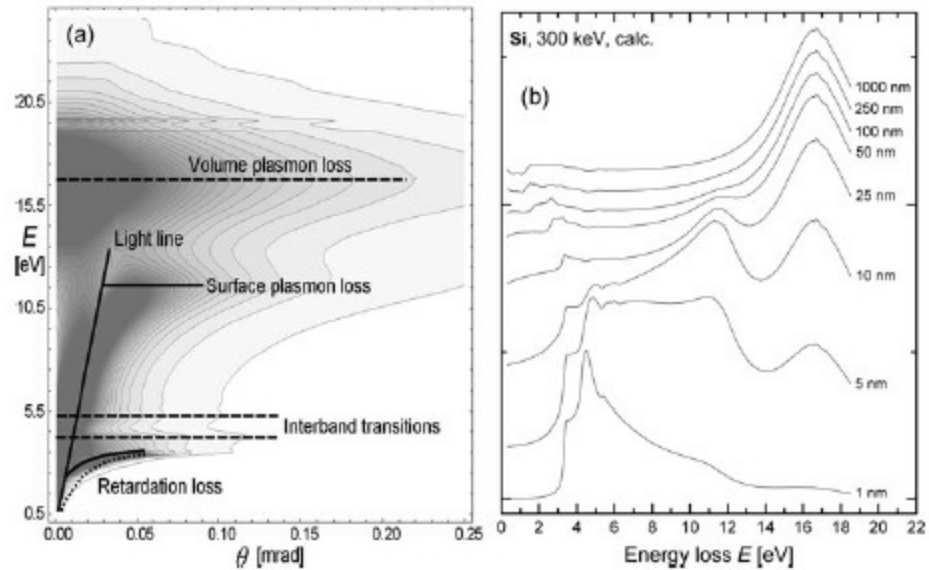
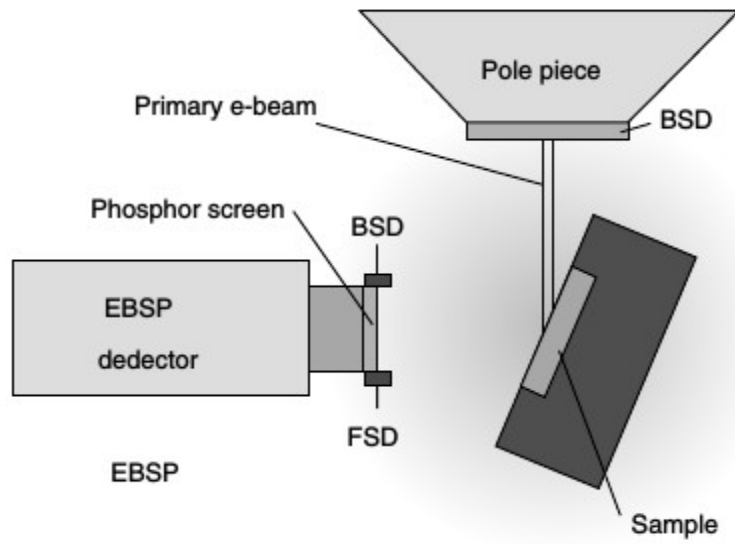
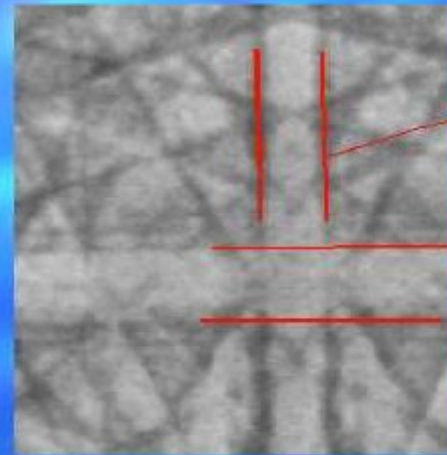
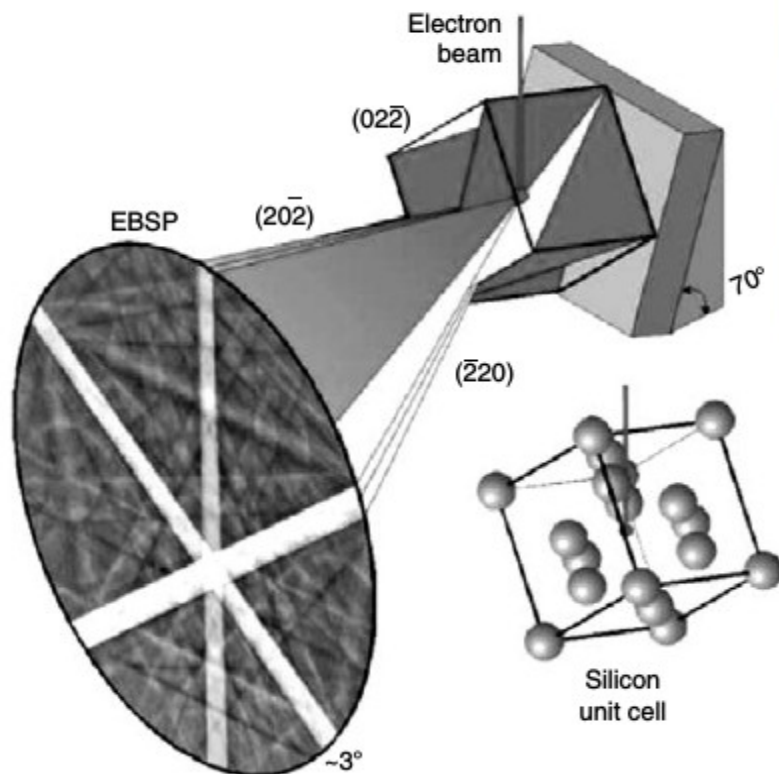


Fig. 3.26 (a) Schematic and contour plot (*gray background*) showing the calculated energy loss and angular dependence of intensity for a 50-nm Si specimen and 300-keV incident electrons. (b) Energy-loss spectra calculated from Eq. (3.84) for 2.1-mrad collection semi-angle, 300-keV incident electrons, and various thicknesses of silicon, assuming no surface-oxide layer. The intensities are normalized and the spectra displaced vertically for clarity. Reproduced from Erni and Browning (2008), copyright Elsevier. A computer program for evaluating Eq. (3.84) is described in Appendix B9

EBSD



EBSD



Bright 'Kikuchi' bands correspond to planes in the crystal lattice

Width of bands is dependent upon electron wavelength and lattice plane spacing

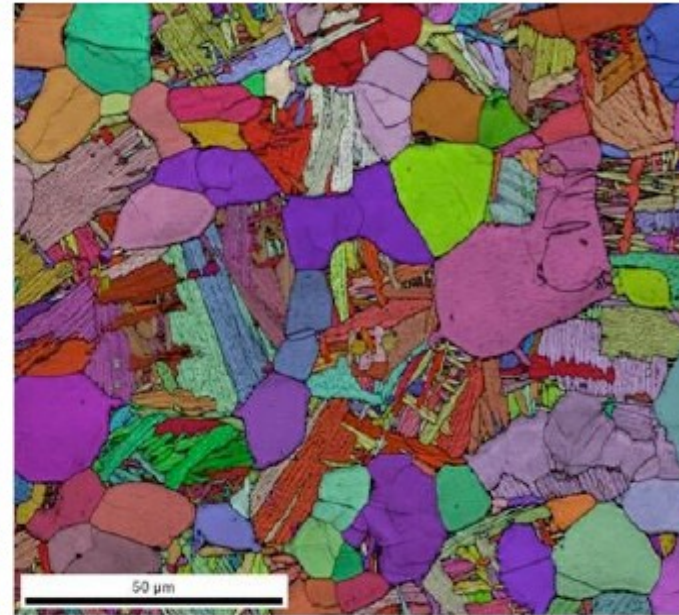
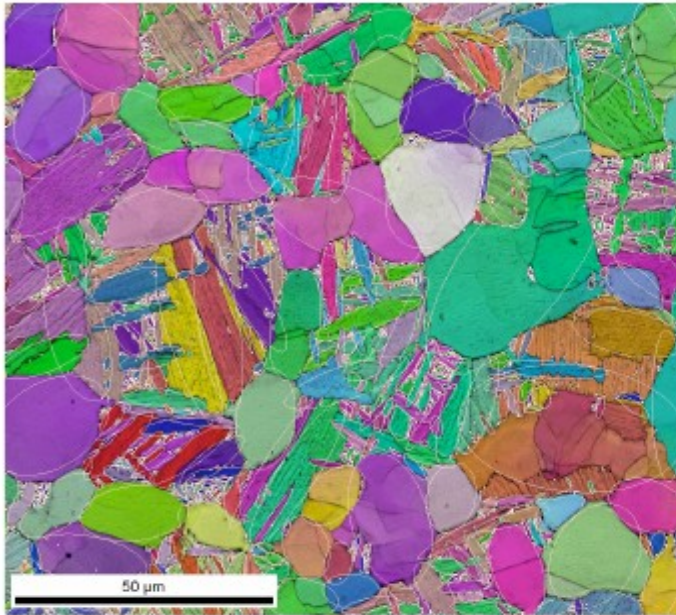
The EBSP contains the angular relationship between the planes, the symmetry of the crystal and orientation information.

Relationship is given by the Bragg equation
 $\lambda = 2d \times \sin\theta$

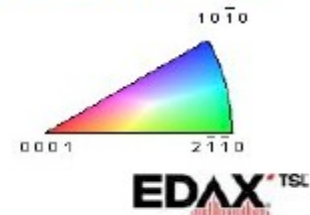
FIGURE 2.8. Electron interaction with crystalline material. (Adapted from [13].)

EBSD

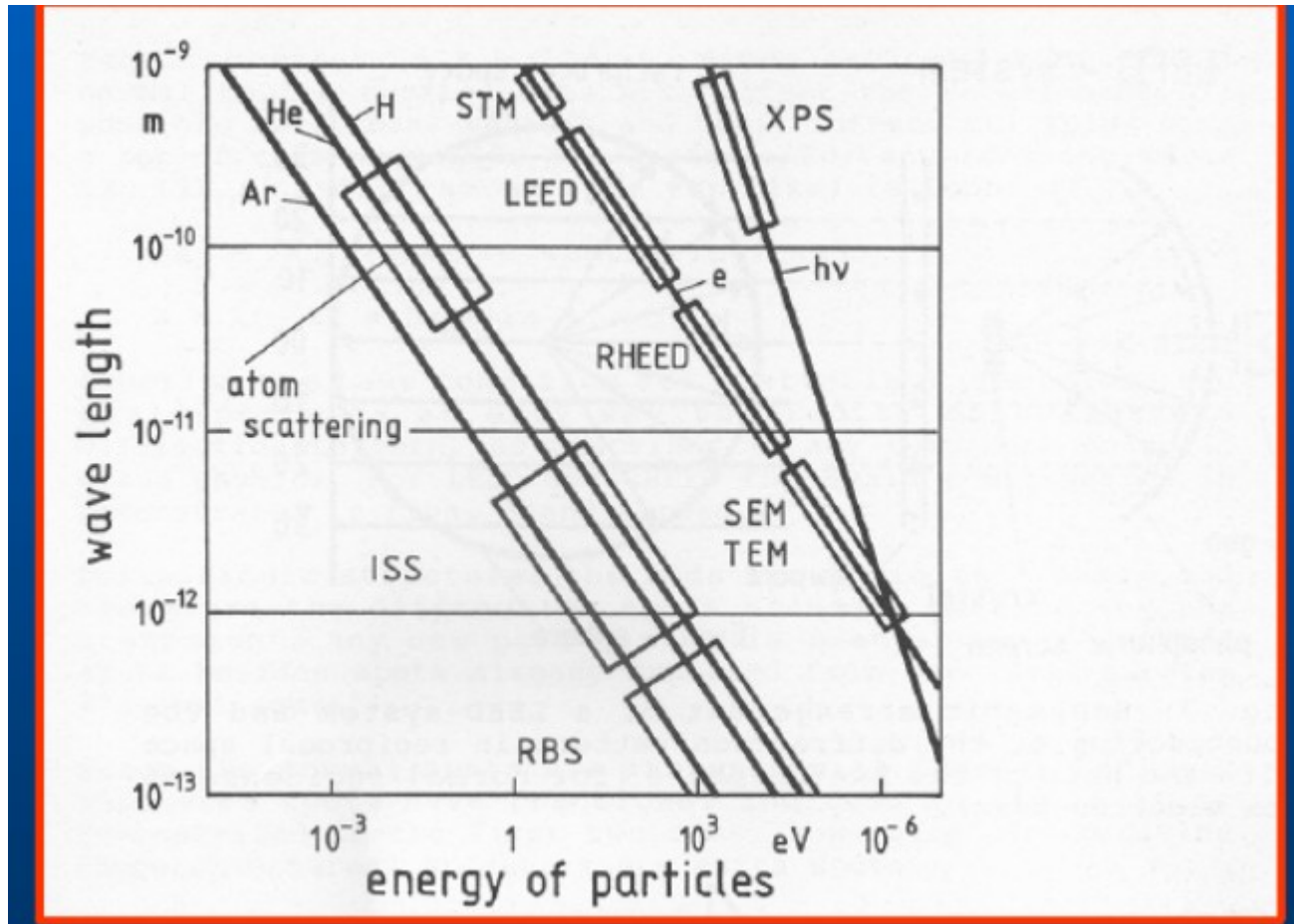
Titanium Grain Structure



Once the grain shape is known, the orientation of the major axis can also be examined to understand growth mechanisms.

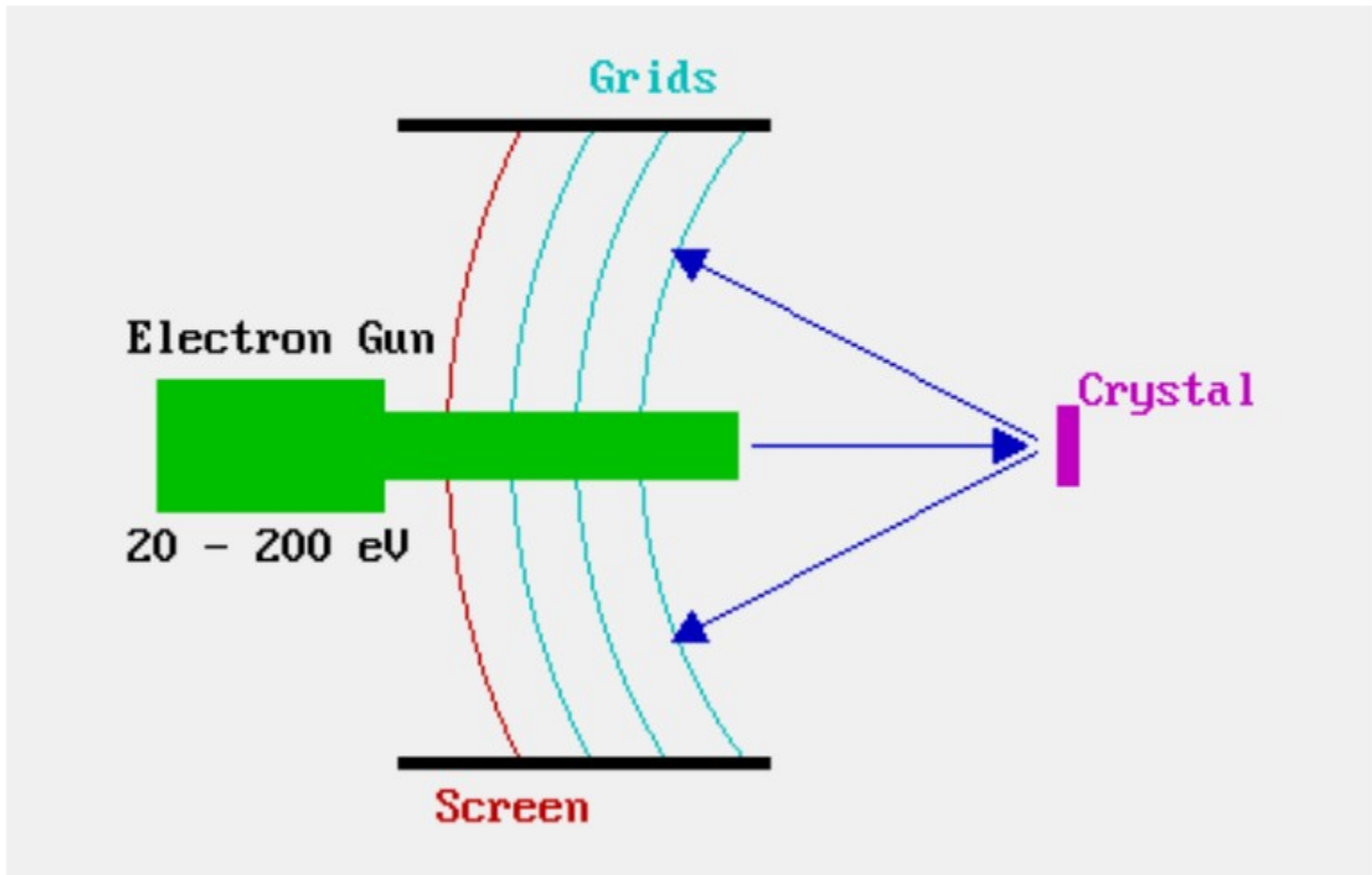


Electron diffraction



Electron diffraction

Schéma LEED



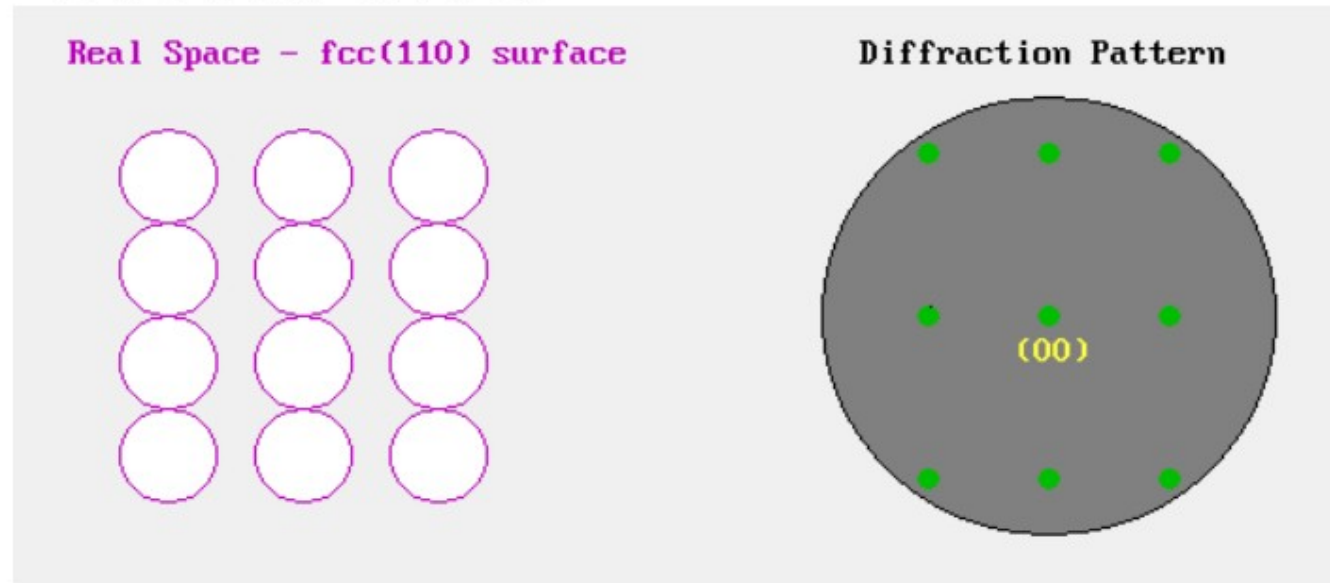
LEED

- Typické energie 20 eV až 200 eV, ve směru normály povrchu
- Kvalitativně:
 - Z pozice spotů lze zjistit také velikost, symetrii, atd. absorbátů na povrchu, lze samozřejmě analyzovat i jen samotný substrát
- Kvantitativně:
 - Přesné pozice atomů lze zjistit z měření intenzit, závislosti I-V, porovnáním s teorií a modely
 - Profil intenzit jednotlivých spotů

Co se stane pokud zvýšíme energii elektronů

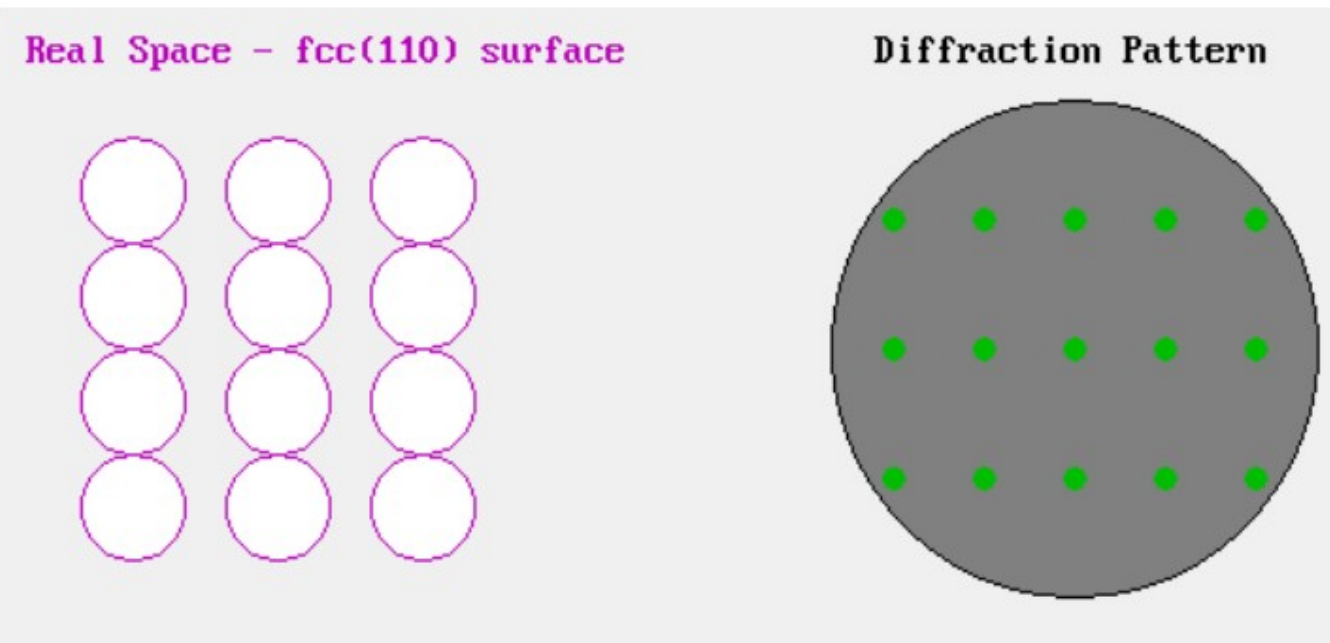
- Nízká

- Zde jen $n = 1$ pro úhly θ , viz podmínka pro vznik maxim.



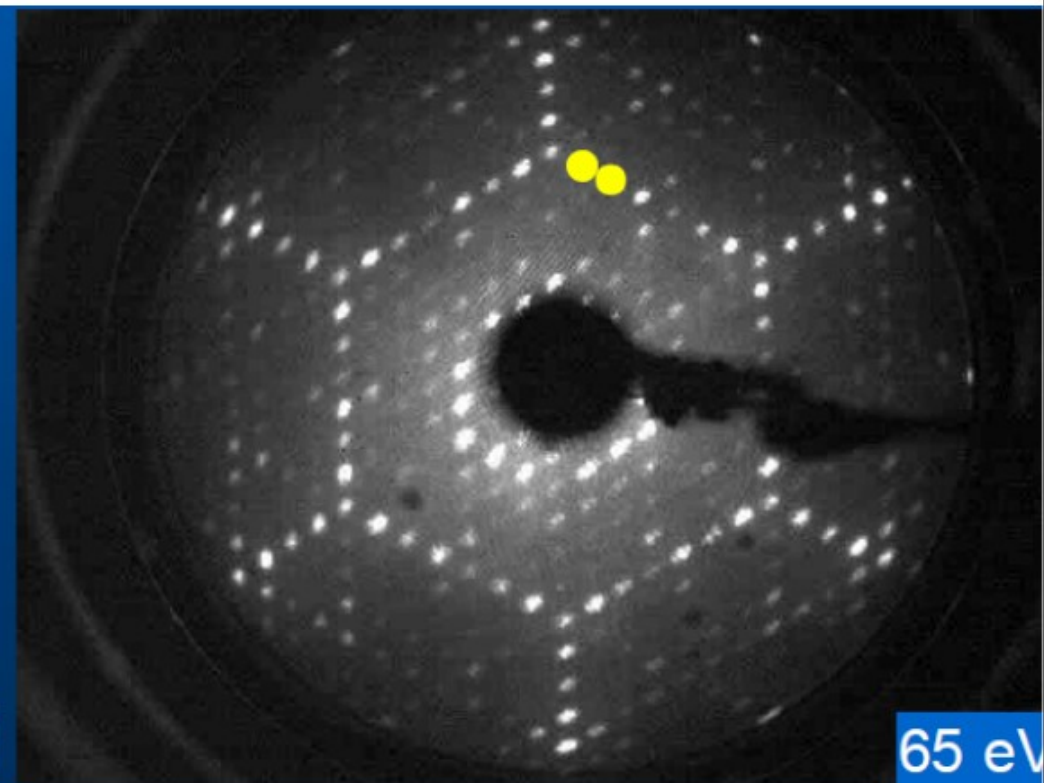
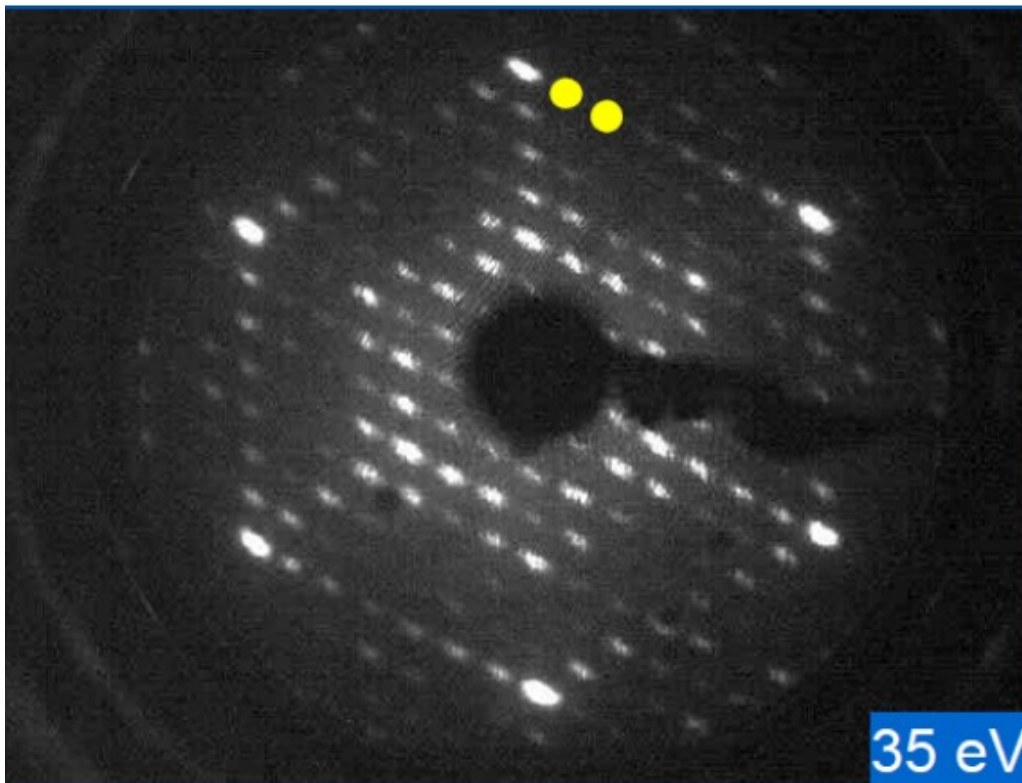
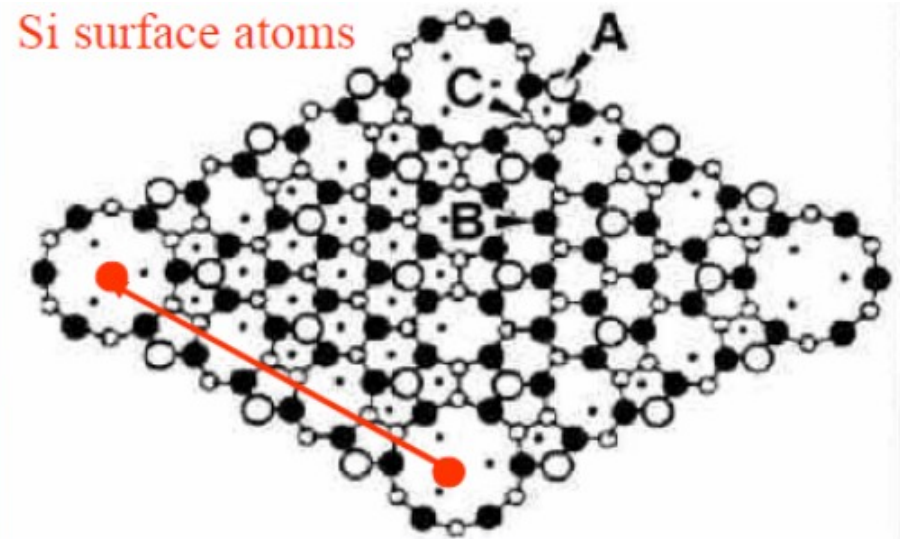
- Vyšší

- (dvojnásobná)


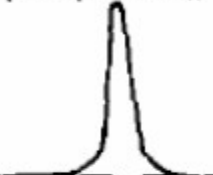



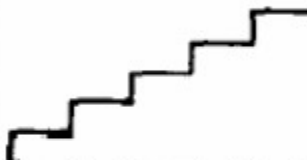




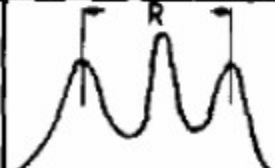
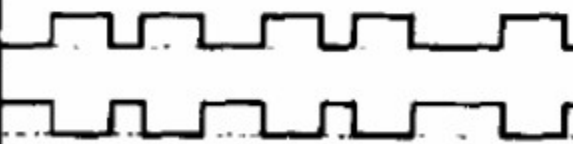

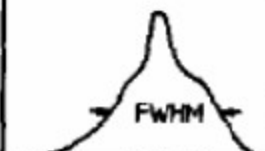



Electron diffraction

Si 7x7

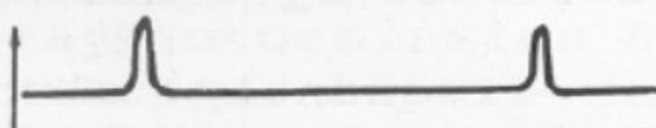
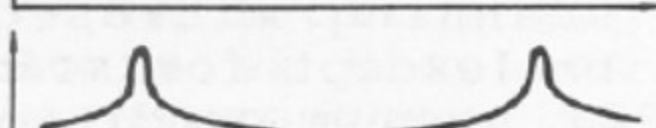
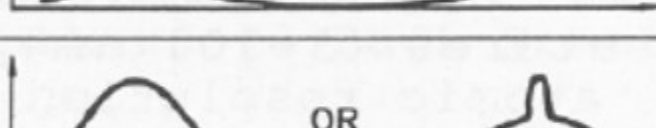

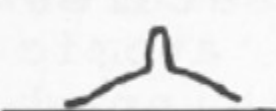
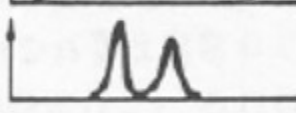
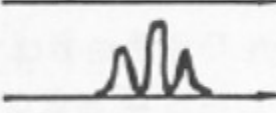
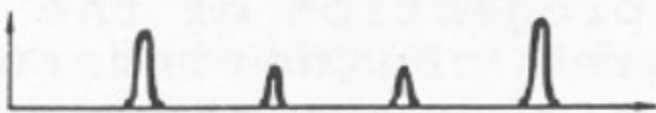
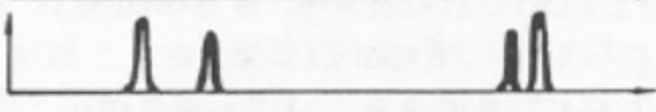

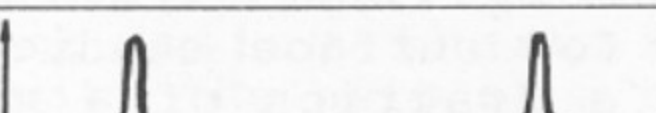


Electron diffraction

information extracted from LEED spots			
spot shape	spot profile	surface structure	
a 			ideal surface
b 			regular steps
c 			random steps
d 			regular size or regular distance islands
e 			random size and distance islands

Gronwald and Henzler M. Surf. Sci. 117 (1982)

Electron diffraction

CLASSIFICATION OF SURFACE DEFECTS		
DIM.	EXAMPLES	EFFECT ON SPOT PROFILE
0	POINT DEFECTS THERMAL DISORDER STATIC DISORDER	ARR.:  K_{\perp} DEP. NONE
		RAND.:  NONE
		CORREL.:  MONOT.
1	STEP EDGES DOMAINS DOMAIN BOUND	RAND.:  OR  PER. (STEPS)
		REG.:  OR  NONE (DOMAINS)
2	SUPERSTRUCTURE FACETS	 NONE
		 PER.
3	BULK DEFECTS (MOSAIC, STRAIN)	 MONOT.
	IDEAL SURFACE	 NONE

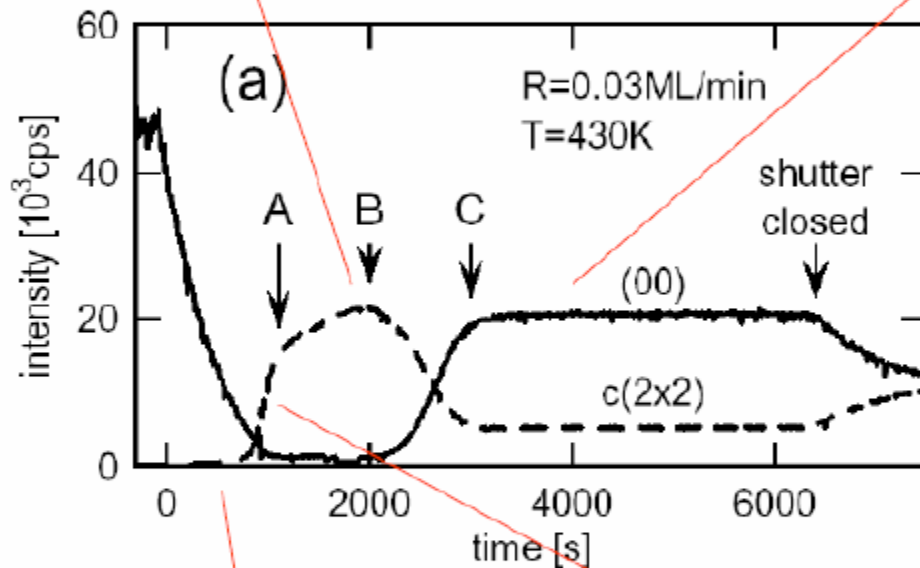
Electron diffraction

Simultaneous Inspection of Several Diffraction Spots

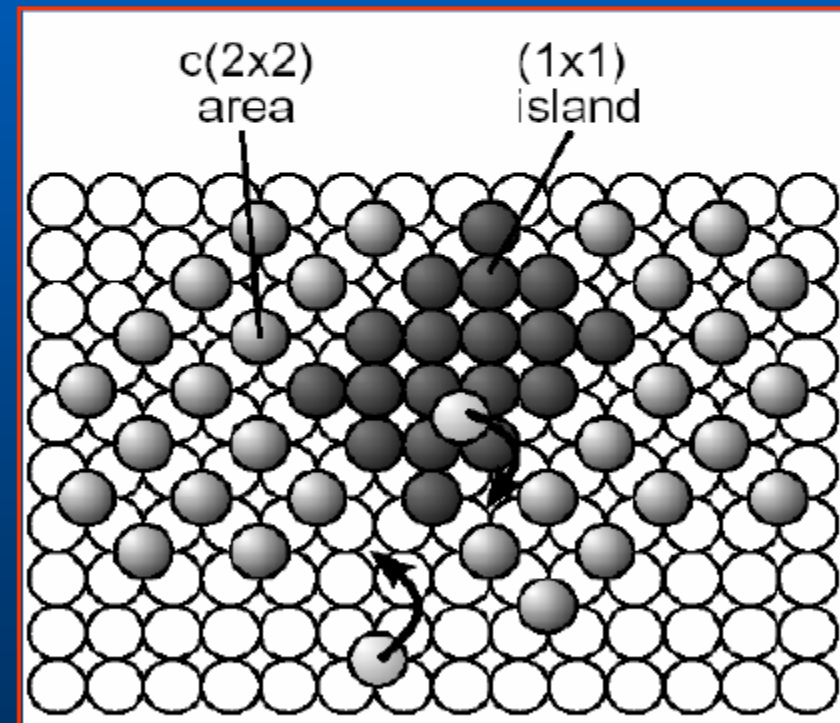
Mg/Ag(100)

perfect order - $c(2 \times 2)$

adsorption – desorption equilibrium



$c(2 \times 2)$ has a higher bonding energy than (1×1) pseudomorphic layer



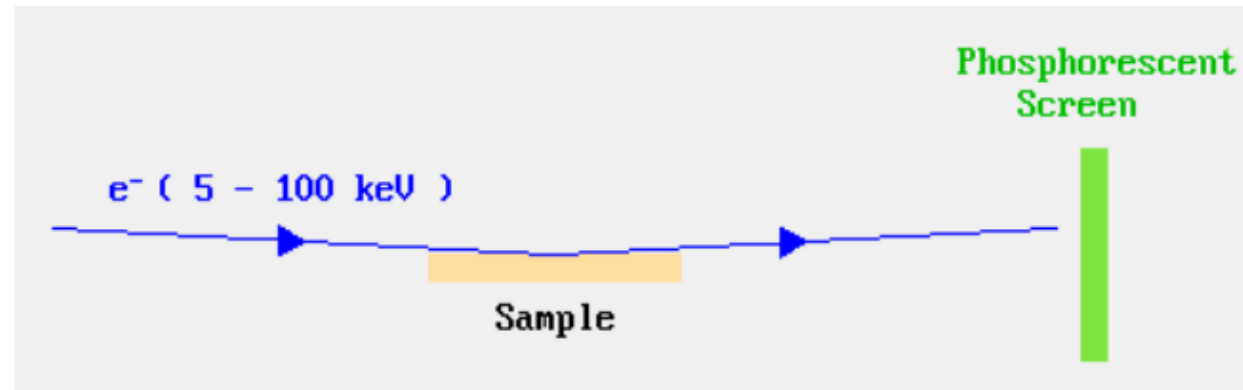
delay in $c(2 \times 2)$ formation due to surface alloying

demixing – $c(2 \times 2)$

Electron diffraction

RHEED

- Typické energie 5 keV až 100 keV,
- Charakteristiky
 - Dopředný rozptyl
 - Úhel rozptylu



Electron diffraction

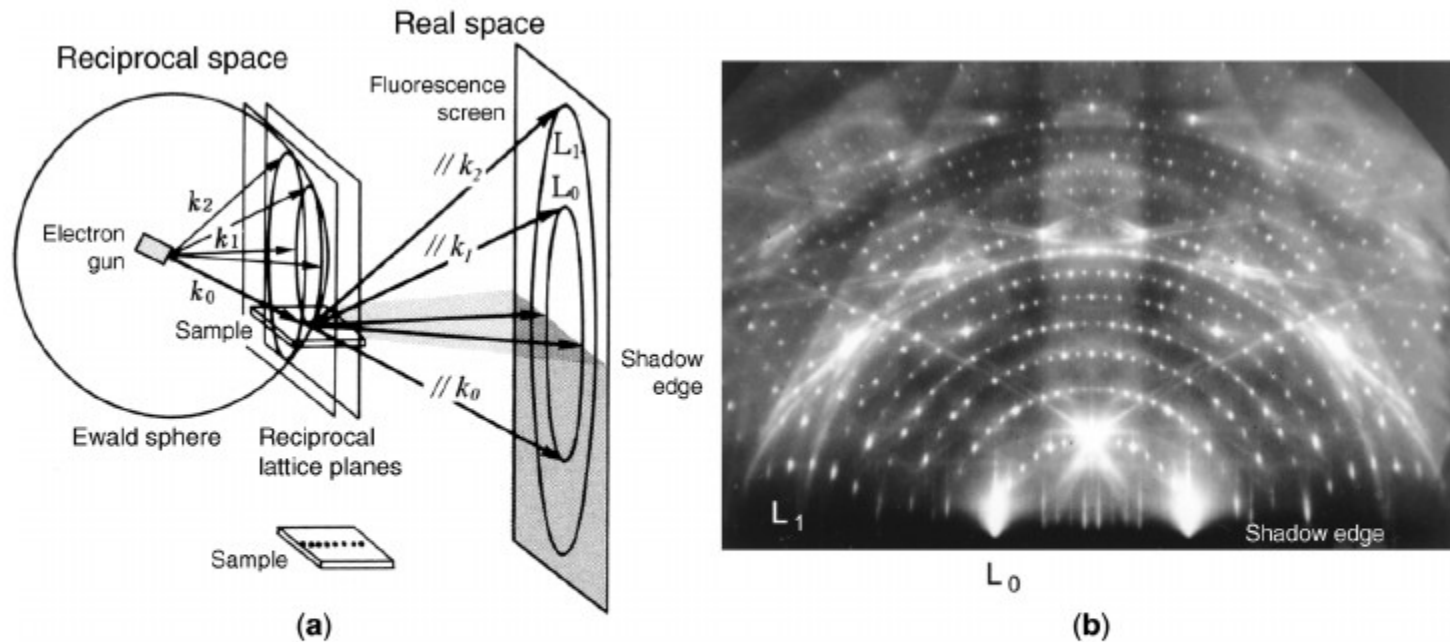


Figure 2. (a) Direct space and reciprocal space of RHEED. (b) RHEED pattern taken from a Si(111)-(7 × 7) reconstructed surface. The electron beam was 15 keV in energy with $[11\bar{2}]$ incidence in azimuth direction and about 3° in glancing angle θ_g to attain a surface-wave resonance condition.

Electron diffraction

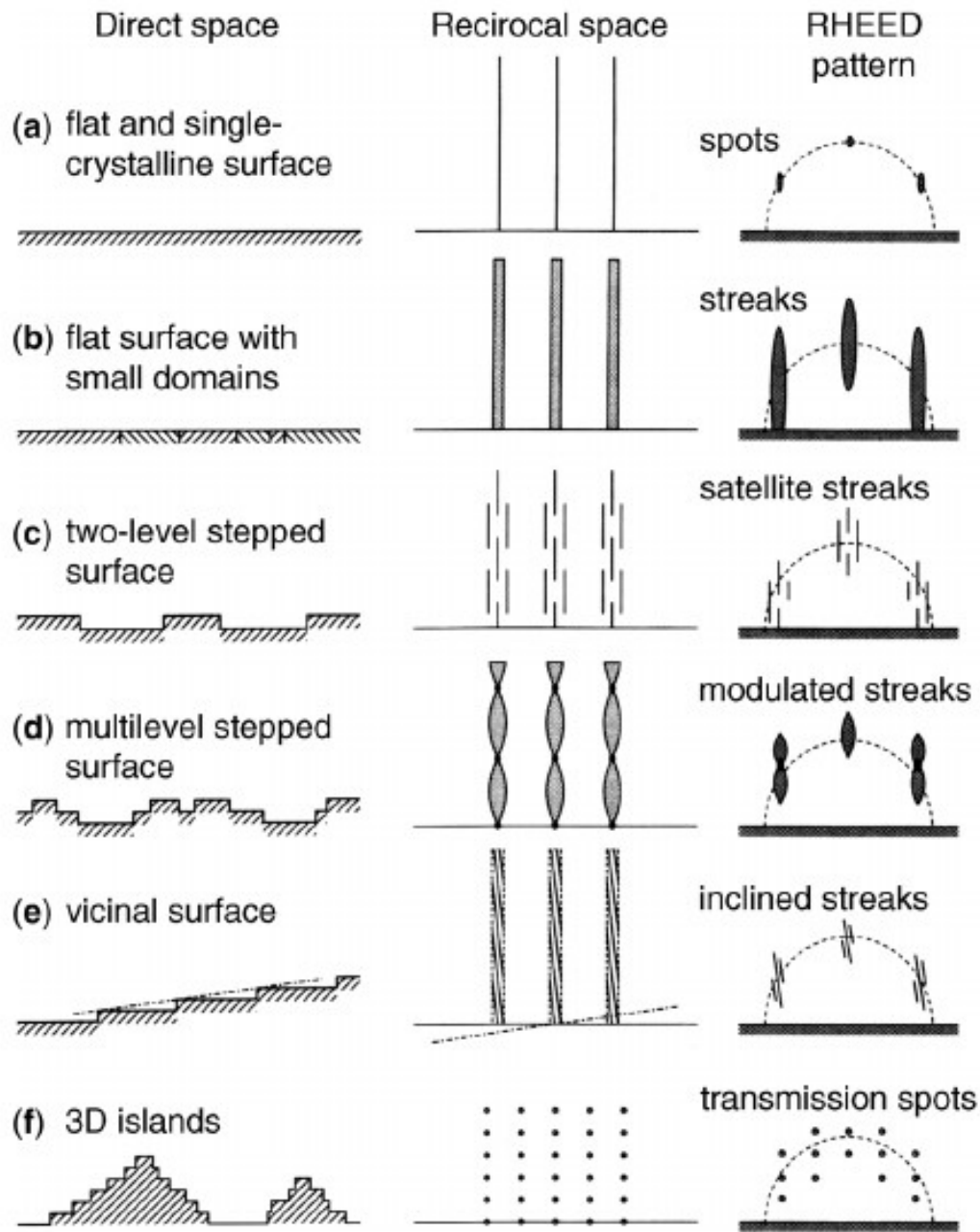


Figure 3. Schematics of various kinds of realistic surfaces, in real-space morphology, in reciprocal space, and their RHEED patterns (courtesy by Yoshimi Horio).

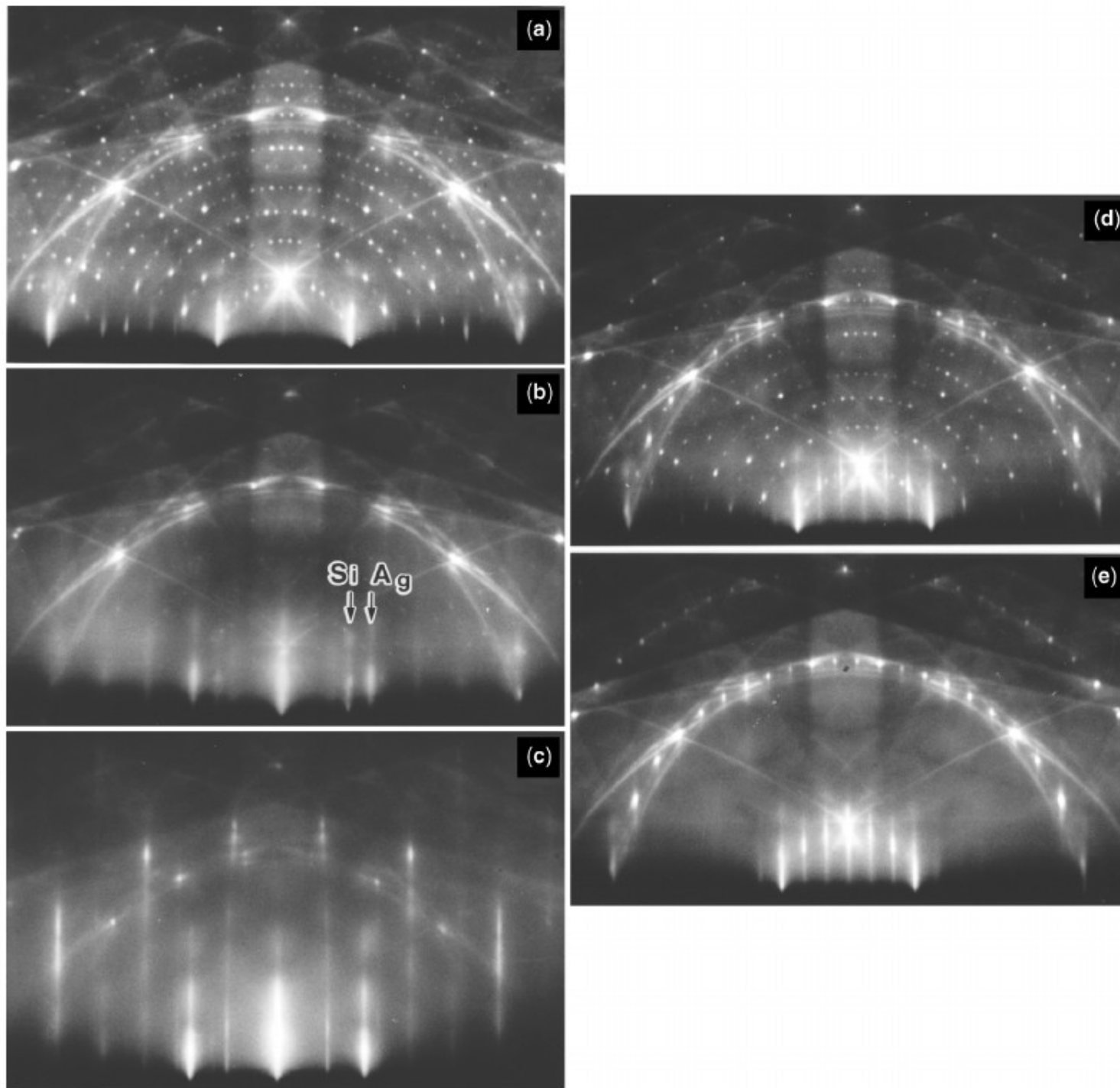


Figure 4. RHEED patterns observed during Ag deposition onto Si(1 1 1)-(7 × 7) reconstructed surface **(a)** at room temperature **(b)(c)** and at 440°C **(d) (e)**. The amount of Ag deposited is **(b)** 1.5 ML, **(c)** 3.0 ML, **(d)** 0.5 ML, and **(e)** 1.0 ML. ML (monolayer) means a single-atomic layer. Reprinted from (Hasegawa et al., 1987), Copyright 1987, with permission from Elsevier.

Electron diffraction

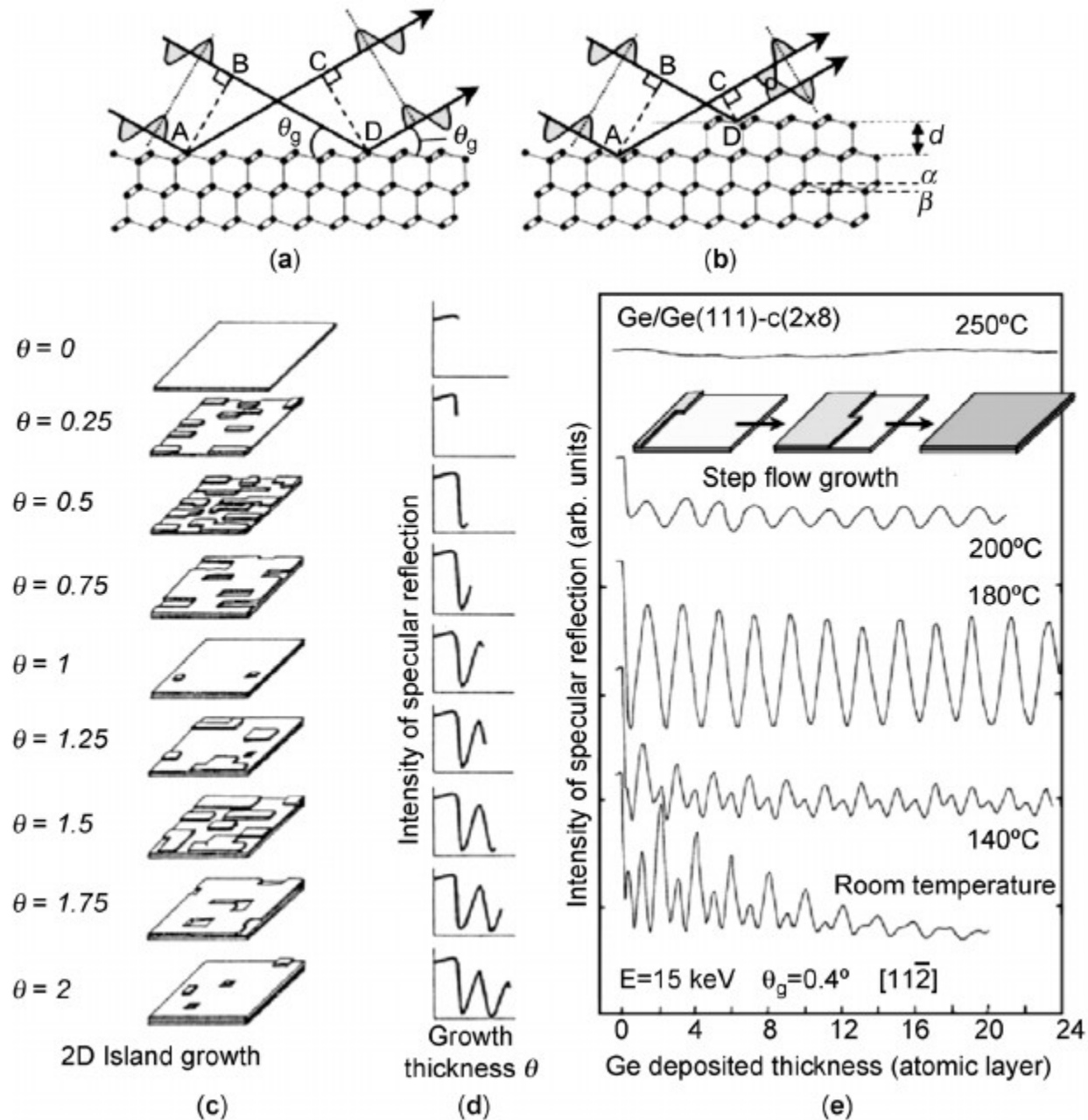


Figure 10. RHEED intensity oscillation and crystal growth monitor. (a) and (b) Specular beam from a flat surface and a stepped surface, respectively. (c) Illustrations showing a 2D-island growth style and (d) the intensity change of specular spot during the growth, reprinted from (Joyce et al., 1986). Copyright 1986, with permission from Elsevier. (e) Experimental data of RHEED intensity oscillations during Ge homoepitaxy on Ge(1 1 1) surface (Fukutani et al., 1992).

Table 1.1 Imaging and analysis techniques employing electron, ion, and photon beams, with estimates of the achievable spatial resolution

Incident beam	Detected signal	Examples	Resolution (nm)
Electron	Electron	Electron microscopy (TEM, STEM)	0.1
		Electron diffraction (SAED, CBED)	10–1000
		Electron energy-loss spectroscopy (EELS)	<1
		Auger electron spectroscopy (AES)	~2
	Photon	X-ray emission spectroscopy (XES)	2–10
		Cathodoluminescence (CL)	
Ion	Ion	Rutherford backscattering spectroscopy (RBS)	1000
		Secondary ion mass spectrometry (SIMS)	50
		Local electrode atom probe (LEAP)	0.1
	Photon	Proton-induced x-ray emission (PIXE)	500
Photon	Photon	X-ray diffraction (XRD)	30
		X-ray absorption spectroscopy (XAS)	20
		X-ray fluorescence spectroscopy (XRF)	
	Electron	X-ray photoelectron spectroscopy (XPS)	5–10
		Ultraviolet photoelectron spectroscopy (UPS)	1000
		Photoelectron microscopy (PEM or PEEM)	0.5
		Ion	Laser microprobe mass analysis (LAMMA)